Title

Advanced Monte Carlo simulations of emission tomography imaging systems with GATE

Journal

Physics in Medicine and Biology, 66(10)

ISSN

0031-9155

Authors

Sarrut, David

Bała, Mateusz

Bardiès, Manuel

et al.

Publication Date

2021-05-21

DOI

10.1088/1361-6560/abf276

Peer reviewed

Published in final edited form as:

Phys Med Biol. ; 66(10): . doi:10.1088/1361-6560/abf276.

Advanced Monte Carlo simulations of emission tomography imaging systems with GATE

David Sarrut[1], **Mateusz Bała**[7], **Manuel Bardiès**[20], **Julien Bert**[18], **Maxime Chauvin**[11], **Konstantinos Chatzipapas**[15], **Mathieu Dupont**[5], **Ane Etxebeste**[1], **Louise M. Fanchon**[16], **Sébastien Jan**[3], **Gunjan Kayal**[11,12], **Assen S. Kirov**[16], **Paweł Kowalski**[8], **Wojciech Krzemien**[8], **Joey Labour**[1], **Mirjam Lenz**[9,10], **George Loudos**[15], **Brahim Mehadji**[5], **Laurent Ménard**[13,14], **Christian Morel**[5], **Panagiotis Papadimitroulas**[15], **Magdalena Rafecas**[21], **Julien Salvadori**[4], **Daniel Seiter**[17], **Mariele Stockhoff**[6], **Etienne Testa**[19], **Carlotta Trigila**[2], **Uwe Pietrzyk**[10], **Stefaan Vandenberghe**[6], **Marc-Antoine Verdier**[13,14], **Dimitris Visvikis**[18], **Karl Ziemons**[9], **Milan Zvolský**[21], **Emilie Roncali**[2]

[1.]Université de Lyon; CREATIS; CNRS UMR5220; Inserm U1294; INSA-Lyon; Université Lyon 1, Lyon, France

[2.]Department of Biomedical Engineering, University of California and Dept. of Radiology, UC Davis School of Medicine, Davis, CA 95616 USA

[3.]Université Paris-Saclay, CEA, CNRS, Inserm, BioMaps, Service Hospitalier Frédéric Joliot, F-91401, Orsay, France.

[4.]Department of Nuclear Medicine and Nancyclotep molecular imaging platform, CHRU-Nancy, Université de Lorraine, 54000, Nancy, France.

[5.]Aix-Marseille Univ, CNRS/IN2P3, CPPM, Marseille, France

[6.]Medical Image and Signal Processing (MEDISIP), Ghent University, Ghent, Belgium

[7.]Jagiellonian University, Krakow, Poland

[8.]High Energy Physics Division, National Centre for Nuclear Research, Otwock-Świerk, Poland

[9.]FH Aachen University of Applied Sciences, Juelich, Germany

[10.]Faculty of Mathematics and Natural Sciences, University of Wuppertal, Wuppertal, Germany

[11.]CRCT, UMR 1037, INSERM, Université Toulouse III Paul Sabatier, Toulouse, France

[12.]SCK CEN, Belgian Nuclear Research Centre, Boeretang 200, Mol 2400, Belgium

[13.]Université Paris-Saclay, CNRS/IN2P3, IJCLab, 91405 Orsay, France

[14.]Université de Paris, IJCLab, 91405 Orsay France

[15.]Bioemission Technology Solutions (BIOEMTECH), Mesogeion Av. 387, Athens, Greece

[16.]Department of Medical Physics, Memorial Sloan Kettering Cancer Center, New York, NY, 10065, USA.

[17]Department of Medical Physics, University of Wisconsin-Madison School of Medicine and Public Health, Madison, WI, 53705, USA

[18]LaTIM, INSERM UMR 1101, IBRBS, Faculty of Medicine, Univ Brest, 22 avenue Camille Desmoulins, 29238, Brest, France.

[19]Univ. Lyon, Univ. Claude Bernard Lyon 1, CNRS/IN2P3, IP2I Lyon, F-69622, Villeurbanne, France.

[20]Cancer Research Institute of Montpellier, U1194 INSERM/ICM/Montpellier University, 208 Av des Apothicaires, 34298 Montpellier cedex 5, France.

[21]Institute of Medical Engineering, University of Lübeck, Lübeck, Germany.

Abstract

Built on top of the Geant4 toolkit, GATE is collaboratively developed for more than 15 years to design Monte Carlo simulations of nuclear-based imaging systems. It is, in particular, used by researchers and industrials to design, optimize, understand and create innovative emission tomography systems. In this paper, we reviewed the recent developments that have been proposed to simulate modern detectors and provide a comprehensive report on imaging systems that have been simulated and evaluated in GATE. Additionally, some methodological developments that are not specific for imaging but that can improve detector modelling and provide computation time gains, such as Variance Reduction Techniques and Artificial Intelligence integration, are described and discussed.

1. Introduction

GATE is an open-source, community-based software effort relying on the Geant4 toolkit [4] dedicated to Monte Carlo simulation in medical physics. GATE is about 15 years old and evolves a lot through users' contributions. It was initially focused on nuclear imaging [18; 66; 159; 182], then expanded to external and internal radiotherapy [68], dosimetry [162] and hadrontherapy [56]. The simulated physics is managed by the Geant4 Monte Carlo kernel in charge of tracking particles in matter and processing physical interactions. On top of Geant4, GATE gathers multiple developments that facilitate medical physics simulations. Indeed, numerous clinical, preclinical, and prototype positron emission tomography (PET) and single photon emission compute tomography (SPECT) scanners were simulated and confronted with experimental data.

Since the initial 2004 OpenGATE collaboration article, emission tomography systems have changed dramatically [199] with improved time-of-flight (TOF) methods, better detection systems based on silicon photomultipliers (SiPMs), long axial field of views (FOV), multi-headed systems, etc. At the same time, Monte Carlo simulation also had to evolve to support those developments. This type of simulation remains the gold standard for design, optimization and assessment of imaging systems, and serves to estimate their performance, to optimize acquisition parameters, and to design reconstruction algorithms.

Since then, no synthesis of emission tomography (SPECT, PET, Compton camera) capabilities of GATE has been published. The goal of this paper is to review the current gate capabilities and limitations for simulating emission tomography imaging systems. The article is organized in the following way: section 2 describes the recent developments for detector simulations, section 3 gives more details about validated simulated imaging systems, and finally section 4 reports on additional developments not specific to emission tomography yet helpful to the field.

2. Detector developments

In the following, we describe the main modules recently developed or updated for simulation of modern emission tomography systems. the first subsection summarizes the two main modes of simulation, then, we describe optical photon tracking, cerenkov-based TOF and Compton camera modules.

2.1. Principal simulation modes

In nuclear imaging, events are usually detected by collecting scintillation photons emitted after energy deposition of high-energy gamma photons in inorganic crystals (LYSO‡, LSO§, BGO‖, etc) using photodetectors such as photomultiplier tubes (PMT), avalanche photodiodes (APDs) or SiPMs [150]. There are two modes that can be used in GATE to simulate this detection stage.

The first mode consists in full Monte Carlo tracking of the emitted optical photons. In such simulations, precise definition of the crystal optical surfaces is crucial to obtain a realistic light distribution. While it is useful to design and to better understand the in-depth behavior of a given detection system, simulating all optical photons leads to long computation times due to the very large number of tracked particles [26]. This first mode will be presented in section 2.2.

In the second simulation mode in GATE, the response of the photodetection components is simulated by a specific module called a *digitizer*. In that case, an analytical model is used to generate detection events from the list of interaction events within the crystal, assuming the number of generated digital pulses is proportional to the number of scintillation photons in the crystal. This *digitizer* converts photon interactions in the crystal into digital counts and assigns time stamps to every event. Numerous parameters are provided to the user who can apply successive signal processing operations to generate a final response adapted to the hardware: pixelated or monolithic scintillator detectors, depth-of-interaction (doi) modelling, dead time, etc. Moreover, various stochastic uncertainties can be added to reproduce the intrinsic resolution of components such as the intrinsic radioactivity of ^{176}Lu in LSO [108], or the intrinsic resolution of a particular scintillator [66].

A specific vocabulary is used: *hits, singles, coincidences*. Individual particle interactions within a detector element (e.g. crystal) are called *hits*, each *hit* containing information about

‡lutetium-yttrium oxyorthosilicate
§lutetium oxyorthosilicate
‖bismuth germanium oxide

the interaction process type, the position, deposited energy, time, the volume where the interaction occurs, etc. The *hits* within the same readout volume are gathered into *singles*. *Singles* are sorted by time-stamp and associated in *coincidences* according to several rules, in particular to handle multiple coincidences where more than two singles are detected within the same coincidence window. In PET imaging, it is common to consider several types of coincidences: the *scatters* (coincidence events resulting from scattered photons inside the subject), the *randoms* (accidental coincidences), the *trues* (coincident detection of the two 511 keV photons coming from the same annihilation event). The sum of those three types are called the *prompts* (total detected coincidences). In reality, the number of *randoms* is not known from experimental data and is estimated by the *delay* coincidences obtained from delayed time coincidence windows [183]. GATE generates all types of coincidences for detailed analysis.

The *digitizers* processes are common to PET, SPECT and Compton camera modules and may be used either online, during the Monte Carlo particle tracking, or offline, after the end of the simulation. In this latter case, the simulation output requires *hits, singles*, and/or *coincidences* data to be saved in root (or python) files that can be post-processed. More details can be found in [39; 183].

2.2. Optical photon tracking and sipm

The precise definition of crystal optical surfaces can be modeled with the *davis look-up table (LUT) surface reflection model*, introduced in GATE since version 8.0 [180]. This model is based on measured surface data obtained by atomic force microscopy. Users can choose between two surfaces, a polished and a rough one. For each surface, four LUTs are available: LSO crystal with no reflector, coupled to teflon through an air interface, esr-air and esr-grease. the models consider optical photon reflection probabilities and directions depending on the incidence angle of the photon on the crystal surface. The models were validated against experimental data. Next step towards finer detector modelling lies in the use of completely customized LUTs. For this reason, a standalone user interface has been developed to allow users to generate LUTs for any surface obtained with a 3D scanning method with a sub-micron resolution with the personalized definition of the intrinsic properties of the scintillator and the coupling medium and a specific reflector attached to the crystal. The LUTDavis model has been validated for several configurations by comparing the experimental and simulated light output of single crystals, with an error of less than 10% [151].

With the *LUTDavis model*, a large monolithic scintillation detector for clinical PET systems was simulated using optical photon tracking. The detector consisted of $50 \times 50 \times 16$ mm^3 LYSO coupled with optical grease to an array of SiPMs (see figure 1). The gamma entrance face was defined with the polished ESR LUT. The crystal sides were defined with an adapted LUT modelling a rough surface with black paint leading to absorption of photons transmitted by the crystal surface. The SiPM readout side was simulated by LUTs that model polished surfaces and take into account the index of refraction of optical grease. Optical simulations were used to optimise the performance of the detector by testing various setups and their influence on the desired performance parameter. It was thus possible to gain

insight into physical processes that are difficult or impossible to measure experimentally, notably ground-truth interaction positions, especially depth-of-interaction. Each influencing factor can be analysed separately as for example the influence of Compton scattered events, the influence of intrinsic ^{176}Lu radiation of the scintillator, the influence of test-equipment, e.g. collimators or housing.

In [181], the focus was set on the spatial resolution influenced by the size of the photodetector pixels, the photon detection efficiency and the number of channels used to read out the sensor array. The outcome of this simulation study demonstrated the high spatial resolution of 0.4 to 0.66 mm full width at half maximum (FWHM) that can be obtained by a monolithic detector under idealized configurations. High Photon Detection Efficiency (PDE) and small pixel sizes improved the resolution, while the number of electronic readout channels could be decreased drastically by summing rows and columns with only a small or no degradation on the spatial resolution. In Decuyper et al. [32; 33] the performance of the detector could further be improved by using artificial neural networks (ANNs) to train the positioning algorithm. The simulation was used to identify and address potential pitfalls related to ANNs which could then be translated to the experimental results.

The simulation of single detector modules does not only require a dedicated surface modelling, but also has to account for the detection of scintillation photons and the subsequent pulse processing inside the photodetector. The increasing use of SiPMs (see section 3) in the context of PET imaging [19; 29; 98] motivated the implementation of specific *digitizer modules* for analogue and digital SiPMs, so that both the complete scanner system and the single detector modules can be simulated.

First, a digitizer module for *analog SiPMs (aSiPMs)* was implemented, allowing to reproduce signals originating from aSiPMs. For each optical photon impinging onto the surface of detection, a pulse has a non-null probability to be generated at a time $t + \Delta t$ considering the PDE, where t corresponds to the time of the detection and Δt accounts for the Single Photon Time Resolution (SPTR). The digitizer also takes into account aSiPM saturation and various sources of noise such as dark counts, crosstalks, afterpulses, after-crosstalks and signal white noise [109].

A second digitizer module was implemented for *digital SiPMs (dSiPMs)*, referring to the Philips Digital Photon Counter (DPC). A DPC sensor tile is subdivided into 16 so-called dies, which comprise four pixels each and are read out independently. In contrast to aSiPMs, this device stores the number of counted photons on the four pixels of a die and a die timestamp for each event. It therefore delivers a completely digital signal. Furthermore, it makes use of a trigger and validation logic in order to reduce the recording of dark counts [34; 46]. This dedicated digitizer currently allows for consideration of the most relevant noise sources (dark noise and optical crosstalk), the PDE of the sensor, and the specific trigger and validation logic. For validation of the model, the probabilities for trigger and validation, determined by [186], have been successfully reproduced [97].

2.3. Cerenkov-based Time-Of-Flight

The use of ultra-fast (10 ps) Cerenkov emission for TOF PET detectors has been investigated extensively as an alternative to traditional time triggering on scintillation photons emitted within tens to hundreds of ns [16; 24; 83; 88; 173]. The potential of Cerenkov light has become the foundation of a paradigm shift in TOF PET, with initiatives such as the 10 ps TOF challenge [89; 90; 163]. The very low number of Cerenkov photons produced by each gamma interaction in the Cerenkov radiator (around 15-20 per photoelectric interaction for BGO) is the main limitation in fully exploiting these photons and warrants thorough studies to better understand their production, transport, collection and conversion into an electric signal. This can only be achieved through detailed simulation, as it is not possible to separate these components experimentally.

GATE has been increasingly used to study Cerenkov emission for its ability to model all aspects of the optical detection chain including the effect of optical surfaces. However, it requires modifications to tag the Cerenkov photons in the *hits* tree and associate them to their parent gamma event [5; 84; 152] and does not include tools for a complete optical analysis. Studies have been reported in two materials: the well-known scintillator BGO, and the novel semi-conductors thallium bromide (TlBr) and thallium chloride (TlCl). In BGO, GATE simulations of the Cerenkov production and transport in the crystal described the direction of the initial Cerenkov photons, as well as the contribution of Cerenkov photons to the detector timing resolution. These simulation studies, in excellent agreement with experimental results, provided a new explanation of the long tails in the timing spectrum observed experimentally in BGO by several groups. GATE simulations in a dual-ended readout BGO detector also elucidated the nature of the time difference between the two crystal ends by identifying the type of photon first detected by the photodetector (Cerenkov or scintillation). In TlBr and TlCl, GATE simulations were used to generate and track Cerenkov photons from the emission point to the photodetector [5]. The number of photons produced and detected per photoelectric interaction was estimated from the simulations, indicating the potential of TlCl as a Cerenkov radiator thanks to its optical properties. Using the simulated photon time stamps, the timing spectrum for different trigger thresholds was computed and confirmed the advantage of TlCl. Good agreement was obtained between simulations and experiments, with an overestimation of the number of detected photons of 12% [5].

2.4. Compton camera modules

The recent GATE Compton camera module (CCMod) [39] provides a framework where different Compton camera configurations can be simulated and facilitates comparison between the performance of different prototypes in medical experimental settings such as hadron therapy monitoring or nuclear medicine. CCMod is designed to reproduce the response of most common configurations in medical applications composed of a *scatterer* and an *absorber* detectors working in time coincidence [41]. However, it can be adapted to accommodate other designs such as one single detector layer system that acts as scatterer and absorber at the same time [96; 105; 113; 116] frequently employed in homeland security applications.

In CCMod, volumes defined as detector layers act as Geant4 sensitive detectors. The detector response (the list of *singles*) is simulated by applying sequentially a chain of digitizer modules to the stored information of particle interactions. The same data structure as in SPECT and PET systems is employed so that digitizer modules may be applied interchangeably to all three types of imaging devices. Since in Compton cameras different detector layers have usually different roles and characteristics, digitizer modules that can be applied independently to each detector layer have been included. *Singles* are sorted into coincidences using the sorter developed for PET systems [183]. Additional options have been included for CCMod such as allowing only *singles* in a specific detector layer (absorber) to open its own time coincidence window. Besides, different criteria for coincidence acceptance are available such as requiring at least one single in each detector type. Since, in a Compton camera system, the order of the *singles* within each coincidence determines the estimated cone surface where the source is located, a dedicated coincidence processor has been included for coincidence sequence reconstruction. At each step of this processing, from interactions to cone information, corresponding data output is available. This recent extension of GATE [39] has been successfully validated against experimental data and employed to predict the performance of prototypes under construction (see section 3).

3. Simulation of imaging systems and applications

This section reviews the emission tomography imaging systems that were simulated and, at least partially, validated against experimental data in GATE. In addition to detector development, and since the very first version, GATE has been used to simulate complete clinical and preclinical imaging systems. Efforts have been made to provide comparison against experimental data and improve the simulation when discrepancies have been found. The tables 1 and 2 list some studies and the associated clinical and preclinical imaging systems (some are illustrated figure 2). Most systems were PET scanners and, to a lesser extend, SPECT devices. CCMod in GATE is very recent [39] and only one validation against experimental data has been reported to date. Most of the evaluation methodologies were based on NEMA protocols and compared Noise Equivalent Count Rate (NECR), sensitivity, resolution, etc between simulated and experimental data. In the following we described some more recent studies, focusing on recent developments such as the use of SiPMs or TOF.

Philips Vereos Digital PET/CT.

In [158], a detailed model of the Vereos DPC-PET was proposed. This PET device, introduced in 2013, is one of the first PET/CT using SiPM detectors, together with, the GE Dicovery MI PET/CT in 2016 and the Siemens Biograph Vision in 2018. On such systems, the location of β^+ annihilation is improved by the use of increase TOF resolution due to the use of SiPMs (210-378 ps). Moreover, the DPC system provides 1:1 coupling between the crystal array and the SiPM array, contributing to decreases uncertainty in the interaction position and to improve the image resolution.

The GATE model of the Vereos described the hierarchical structure of all the detection modules, for a total of 23,040 LYSO scintillator crystals ($4 \times 4 \times 19$ mm^3). The complete digitization chain was simulated including background noise (natural radioactivity of ^{176}Lu in the crystals), dead time and pile-up, temporal resolution and detector quantum efficiency. The model has been evaluated following NEMA NU 2-2018 guidelines, including NECR, scatter fraction, TOF and energy resolution, sensitivity and spatial resolution. The authors reported very good agreement between experiments and simulations for clinical activity concentrations, with differences at maximum lower than 10%, concluding that the proposed GATE model can be used to very accurately reproduce PET images from Vereos system.

PET2020 long axial FOV PET.

In [1; 198] a long axial FOV PET scanner was simulated in GATE. Each ring consists of 36 detector modules made up of $50 \times 50 \times 16$ mm^3 monolithic LYSO crystals. The system has an inner diameter of 65 cm. GATE was used to study the effect and advantage of axial lengths between standard 20 cm, 1 m and 2 m long systems, covering the whole human body versus a coverage of only head-to-hip. A 104 cm long system was 16 times more sensitive than a system with 20 cm axial length (1 m long uniform phantom). The effect of axial splitting of the detector rings to increase the FOV was also studied, in turn for sensitivity as well as an adaptive system bore that allows a sensitivity gain and advantages in spatial resolution due to the reduced acolinearity effect. The study showed that for objects shorter than 1 m the sensitivity gain of a 2 m scanner is limited while the detector cost is doubled compared to the 1 m system. Axial spreading is possible (at the expense of a loss in sensitivity) and an adaptive system bore can be realized by the camera aperture principle.

CaLIPSO brain PET.

The CaLIPSO PET scanner [80] is a detector concept dedicated to human brain studies aiming at providing high detection efficiency with 1 mm^3 spatial resolution and Coincidence Time Resolution (CTR) of about 150 ps. First, the prototype uses a liquid Time Projection Chamber (TPC, see figure 4), where an elementary cell of the PET imager is filled with trimethyl bismuth (TMBi). Electrons and Cerenkov light are produced in the TMBi by γ interactions. Then, Micro-Channel Plate PMTs (MCP-PMT) are used to detect the Cerenkov light with an excellent time resolution (85 ps FWHM). The electrons produced during the γ interactions drift along an electric field and are collected by a pixelated detector of mm^2. Ionization drift time allows to estimate depth of interaction with 1 mm precision [22; 139; 207]. Due to fast Cerenkov light emission, time resolution of CTR close to 150 ps (FWHM) is expected. This makes possible to use TOF technique to improve signal to noise ratio in final images.

Simulation of this full size PET scanner was performed. As illustrated in figure 5, a cubic shape was used to minimize dead zones and to simplify the manufacturing process. The CaLIPSO is composed of 4 sectors of 5×6 elementary modules. The acquisition FOV are 354 mm (axial) and 307 mm (radial). TMBi is encapsulated within a transparent sapphire window coupled to the MCP-PMT with optical gel. The read-out ionization pad structure is also integrated. The GATE digital detection model used dedicated parameterized modules to simulate the detector response for the ionization and light signal readout. These

semi-analytic models were calibrated using detector prototypes. The first estimation of the non-paralyzable dead time was 3.5 μs, corresponding to mean drift time and the shaping time for electronics readout. Estimated spatial resolution of reconstructed images was 1.1 mm in the complete scanner FOV and sensitivity was 17 kcps/MBq.

J-PET long axial FOV PET with plastic scintillators.

J-PET is a PET system based on plastic scintillators allowing for a cost-effective total body solution [118-120; 199]. The J-PET prototype scanner with a long axial FOV built of axially arranged plastic scintillator strips was simulated in GATE [82]. Three diameters of the scanner (75, 85 and 95 cm), three lengths (20, 50 and 100 cm) and two thicknesses T (4 and 7 mm) of scintillators were simulated for both single- and double-layer geometries. Spatial resolution was simulated for three readout solutions: (1) vacuum PMT, (2) SiPM matrices and (3) SiPM readout with an additional layer of Wavelength Shifting (WLS) strips. The WLS were arranged perpendicularly to the scintillator strips, allowing for the determination of the photon interaction point along the tomograph axis, based on the distribution of amplitudes of light signals in WLS strips. The spatial resolution, sensitivity, scatter fraction and NECR were estimated according to the NEMA-NU-2 protocol, as a function of the length of the tomograph, the number of detection layers, the diameter of the tomographic chamber and for various types of applied readout. For the single-layer geometry with a diameter of 85 cm, a strip length of 100 cm, a cross-section of 4 mm × 20 mm and SiPM with an additional layer of WLS strips as the readout, the spatial resolution FWHM in the centre of the scanner was estimated to 3 mm (radial, tangential) and 6 mm (axial). For the analogous double-layer geometry with the same readout, diameter and scintillator length, with a strip cross-section of 7 mm × 20 mm, a NECR peak of 300 kcps was reached at 40 kBq/cc activity concentration, the scatter fraction was estimated to be about 35% and the sensitivity at the centre amounts to 14.9 cps/kBq.

TRIMAGE: trimodality imaging for schizophrenia.

A novel dedicated trimodality (PET/MR/EEG) imaging prototype for schizophrenia was developed within the TRIMAGE project. The brainPET insert was modelled and extensively evaluated with GATE. In [35], several geometrical phantoms were implemented, covering realistic imaging situations. The simulated PET model was evaluated for its performance (spatial resolution, sensitivity and count rate) according to the NEMA standards. Figure 6 depicts the modelled scanner alongside with the NU 2-2001 sensitivity phantom [188] and the PRESTO reconstructions of the NU2-1994 Image Quality (IQ) phantom. Spatial resolution varied between 2.34 mm and 3.66 mm (FWHM) axially moving radially 10 to 100 mm from the center of the FOV. The simulated coincidence efficiency (i.e. the sensitivity) for a point source positioned at the center of the FOV was 61 cps/kBq. To assess the count rates, a solid, cylindrical phantom made of polyethylene (density 0.96 ± 0.1 g/cm^3) with dimensions of 70 mm in length and 25 mm in diameter was used. The phantom was placed at the center of the axial and transaxial FOV of the modelled scanner. A cylindrical hole of 3.2 mm diameter was drilled parallel to the central axis of the cylinder, at a radial distance of 10 mm from the center. The line source insert was a clear polyethylene plastic tube 60 mm in length, filled with 5 to 11 kBq/mL of ^{18}F and threaded through the hole in the

phantom for 1000 s measurement time. The NECR showed a peak above 1.8 Mcps at 250 MBq.

The γ-eye SPECT camera.

In [145], the γ-eye, a small FOV preclinical scintigraphic camera was extensively validated. The γ-eye is produced by BIOEMTECH and is suitable for in-vivo molecular imaging of radiolabeled biomolecules providing a screening tool for dynamic pharmacokinetics studies [49]. The γ-eye detector was simulated with GATE and evaluated for its spatial resolution and sensitivity properties comparing experimental and simulated data. All of the appropriate electromagnetic and physical processes were included, while no cuts or variance reduction techniques (VRT) were applied. A maximum difference, equal to ≈ 16%, on spatial resolution observed, at 7.5 mm distance (5.85 mm experimental value versus 4.9 mm simulation value). In the case of sensitivity, the difference recorded in zero mm source-to-collimator distance (57 cps/MBq versus 63 cps/MBq) was ≈ 10.5%. For all the other distances the difference in sensitivity was lower and very close to the mean value of 56 cps/MBq.

THIDOS compact mobile γ-camera for absorbed radiation dose control in molecular radiotherapy

The THIDOS project aims to the optimization of the individualized patient dosimetry in radioiodine therapy of thyroid diseases by the development of new instrumental and methodological approaches to strengthen the control of the absorbed dose by reducing the uncertainties associated to dose calculation. In that framework we are developing a high-resolution compact and mobile planar γ-camera with a 10 × 10 cm^2 field of view for use at the patient bedside. The goal is to improve the individual quantitative assessment of the distribution and biokinetics of radioiodine in target regions and organs-at-risk before and after treatment administration. In [190], the design of the high-energy parallel-hole tungsten collimator was optimized using GATE and an XCAT 3D voxelized phantom with realistic background and thyroid gland ^{131}I distributions in order to improve quantification of small targets (nodules or tumor remnants) as shown in fig. 7. The camera was fully modelled and a specific study was carried out on the energy and spatial distributions of scattered and penetration events inside the collimator. The best compromise in terms of contrast and signal-to-noise ratio on nodules of various sizes was achieved with a 5.5 cm thick collimator with 1.1 mm hexagonal holes and 0.75 mm thick septa, which allows to minimize the partial volume effect, while reducing both scattered and penetration events (effective septal penetration less than 7.5%). The expected spatial resolution (2 mm FWHM) and efficiency (1.24×10^{-5}) for a ^{131}I source set a 5 cm from the collimator were found to be in good agreement with the experimental results.

MACACO Compton Camera prototype.

In [39], the first version of MACACO (Medical Applications CompAct COmpton camera) prototype [125] built at IFIC-Valencia, was employed for the validation of GATE CCMod against experimental data. This prototype is based on multiple (2-3) layers of $LaBr_3$ monolithic crystals coupled to SiPMs. A system configuration of two layers separated by 50 mm was considered. The crystal sizes were 27.2 × 26.8 × 5 mm^3 and 32 × 36 × 10

mm^3 for the first and second layer respectively both coupled to SiPM arrays with active area pixels of 3×3 mm^2. The first layer was based on four Hamamatsu MPPC S11830-3340MF monolithic arrays whereas the second one was based on an older version S11064-050P(X1) with larger gaps between the pixels. Passive material of the prototype (boards, holders, etc.) was also included in the simulations. The performance of the system was characterized and compared to simulated data in terms of energy spectra, efficiency, angular resolution and back-projection image onto the plane of the source with good agreement. Hence, the angular resolution measure for 1275 keV incident photons was 13.4 ± 0.2° (simulation) versus 13.5±0.2° (experimental). Relative detection efficiency was slightly overestimated 2.6×10^{-3} (simulated) versus 1.9×10^{-3} (experimental) and consistent results within a 3-sigma interval were obtained for energy spectra except for low energies where small differences were observed. These discrepancies were partially caused by the approximations made in the simulation of the experimental discriminator threshold at SiPM pixel level in the digitization process which allow us to avoid the generation and transport of optical photons.

Other applications in interventional nuclear medicine

As nuclear medicine techniques make rapid advancement in surgery and in interventional radiology, we briefly summarize the current uses of GATE in support of these applications. They include simulations of tomography units and 1D and 2D detectors with the goal either to enhance the extracted diagnostic information or to maximize the therapeutic effect of the procedures. Following is a list of GATE uses in radio-guided surgery, in trans-arterial radioembolization and in real-time PET/CT guided biopsies.

In radio-guided surgery, GATE is used to simulate gamma and beta detection probes [175] and optimize the imaging process. Vetter et al [201] used GATE to evaluate the limits of accuracy of an analytical approach to register a previous 3D SPECT image to the readings from an optically tracked hand-held 1D gamma probe an approach known as freehand (fh) SPECT. Since in fh-SPECT the detector positions are arbitrary and the system matrix is not defined, Hartl et al [60] used GATE to simulate a look-up table (LUT) of detector readings at a predefined grid of probe positions around a ^{99m}Tc source in order to obtain the contribution of each source voxel to the detector readings. A LUT created with GATE was used for the fh-SPECT part of a novel hybrid probe combining fh-SPECT with fh-Fluorescence [194]. The authors used a measured LUT for the optical probe. They commented, that while fluorescence simulations are possible with GATE, the optical LUT computation would be challenging since the opto-nuclear probe is not in direct tissue contact which leads to a dynamic ratio of air and skin contributions [194]. In an another development, the design of a PET-like limited angle tomography system for intraoperative radio-guided imaging was explored using GATE by Sajedi et al [156].

After trans-arterial radioembolization of liver tumours with ^{90}Y microspheres, verification of the correct delivery of the microspheres and voxel-based dosimetry can be achieved by performing ^{90}Y SPECT or ^{90}Y PET scans [9]. Since ^{90}Y is a pure β-emitter, the bremsstrahlung radiation used for SPECT imposes the use of broad energy windows which contain large amounts of scattered radiation. In that case, a different Monte Carlo code (SIMIND) was used to optimize the collimators and the energy window for ^{90}Y SPECT

[154]. ^{90}Y PET is challenging due to the very low positron yield (3.186×10^{-5}) and Strydhorst et al performed a detailed analysis of the sources of quantification error in ^{90}Y PET by separating true coincidences from random and true events caused by the ^{176}Lu LSO crystal activity and by bremsstrahlung radiation in phantom simulations with GATE [184]. The point-spread function (PSF) of a cone beam SPECT collimator and the projections of a NEMA phantom model for SPECT parallel hole, cone beam and multifocal collimators were simulated with GATE to validate the performance of the Utrecht Monte Carlo System (UMCS) iterative SPECT reconstruction package for fast pre-radioembolization imaging with ^{99m}Tc macroaggregated albumin (99mTc-MAA) [37]. GATE was also used for investigating various dosimetry aspects of radioembolization [122; 131; 153].

The specimens from real-time PET/CT guided biopsies are radioactive, allowing measurement of the amount and the distribution of the PET tracer contained in them by radioactivity measurements. This concept has been explored to show that autoradiography (ARG) images of the specimens are quantifiable and can aid evaluating adequacy of the specimens for diagnosis and for genomic profiling as well as investigating the specificity of beta emitting radiopharmaceuticals with high resolution [42; 43; 79; 107]. GATE simulations of the positron transport through liver specimens and gelatin-based specimen models which were used for calibrating the ARG detectors were performed to obtain a gel-to-liver correction factor [42; 79]. Further, an ARG image of the tumour cells in a colorectal cancer liver specimen was simulated from the distribution of tumor cells as established in the pathology slices into which the specimen was sectioned [169], see figure 8.

4. Methodological developments within GATE

In addition to developments dedicated to improve detector modelling, which are detailed in section 2, we briefly review in the following sections recent features added in GATE that help to design emission tomography simulation but are not specific to imaging.

4.1. Towards simpler analysis via Python

Historically, Geant4 and High Energy Physics community are linked to the ROOT CERN framework [15] that allows to efficiently manage and analyse physics data. Since the beginning, GATE also allows to write ROOT files, e.g. detector events or phase space, or use them as input, e.g. use phase space file as a source of particles. Python has become the tool of choice for data analysis with modules such as NumPy [59] or Matplotlib [64]. Since version 9.0, GATE now includes additional options to read/write data in NPY file format [59] that can be processed with Python. Also, ROOT files can be processed in Python with the uproot module [136]. Details about the NPY file format can be found in the GATE user guide ¶ and examples of Python analysis are available on the GateContrib repository+.

Finally, the GATE community recently started a new repository, called GateTools*, that gather Python functions that can be useful for simulation setup and analysis. As example,

¶ https://opengate.readthedocs.io
+ https://github.com/OpenGATE/GateContrib
* https://github.com/OpenGATE/GateTools

it contains tools to convert or resize images in various file formats, to convert DICOM RT structures, to manage phase-space files or analyse dose map, with DVH (Dose Volume Histogram) or gamma-index for example. All tools are available as Python function and as command-line independent scripts. At the time of writing, there are more than twenty different tools. The installation is very easy thanks to conventional Python pip install. Like GATE itself, the code is open-source and community driven. It should evolve in the future thanks to users' contributions.

4.2. Variance Reduction Techniques

Several Variance Reduction Techniques were developed in GATE. Among those useful for emission tomography, we can describe the following: For particles with relatively large mean free path lengths comparatively to voxels size, Woodcock tracking [143] using fictitious interactions can be used to speed up tracking; for SPECT simulation, angular response function (ARF) [36; 160; 174] replaces the detector response by an analytical (or neural network) model providing probabilities of detection in all energy channels; ARF can be combined with fixed forced detection (FFD) that forces the detection of a photon in each detector pixel weighted by the probability of emission (or scattering) and transmission to this pixel [20]. The acceleration of all those approaches can reach one order of magnitude, although it depends on many parameters and on the simulation configurations.

4.3. Positronium source

Positronium is a metastable electron-positron bound state, which is formed approximately up to 40% of the cases in a patient's body before the annihilation. It appears in two quantum modes: *ortho-* and *para-positronium*, which have different physical properties, in particular the ortho-positronium lives three orders of magnitude longer than para-positronium, around: 142 ns versus 0.125 ns, respectively. In the tissue, ortho-positronium mean lifetime strongly depends on the size of intramolecular voids (free volumes between atoms), whereas its formation probability depends on the voids concentration [120]. In a patient's body the formation probability and the mean lifetime are in function of the bio-fluids and bio-active molecules concentration [121]. As it was shown in [120], one can reach the mean lifetime precision of about 20 ps. To measure the positronium lifetime, one needs to use non-pure isotopes emitting prompt gammas.

A set of helper classes was added in GATE for the simulations of the positronium decays. Positronium mean lifetime tomography is one of the examples of a novel PET multiphoton imaging technique proposed recently [119]. The available positronium decay models are: para-positronium two-photon decay, ortho-positronium three-photon decay and the mixed model decay where users can adjust a relative frequency of two possible positronium decays. The implemented model of ortho-positronium decay products angular distribution is described in [71]. All the model parameters are configurable by user with a simple GATE macro. In addition, an emission of prompt gamma with a predefined emission energy can be added. Photon polarization settings are also supported at the macro level. This source enables advanced PET imaging applications such as oxygen sensing for tumor hypoxia [171].

4.4. STL geometry

Thanks to the Geant4 `G4TessellatedSolid` class, tessellated mesh geometries composed of triangle primitives are now available in GATE. Users can import STL (stereolithography) files containing the coordinates of vertices and faces of the meshed surface, and GATE generates the corresponding volume in the geometry. One application of this new kind of geometry has been the modeling of the body contouring limited to cubic shapes allows the gamma camera head to move as close as possible to the phantom/patient model thereby preventing their collision in the GATE environment [74; 75]. Meshes for each segmented volume of interest from the phantom/patient model were generated individually using Python scripts and imported in GATE where individual volumes could be assigned with their respective materials from CT [76; 77]. Figure 9 displays the patient mesh model with the auto-contouring gamma camera motion. Total counts in modeled phantom SPECT images obtained with circular and body contouring gamma camera motion with same acquisition parameters revealed a relative difference of around 2.5% and 12% for ^{177}Lu and ^{131}I respectively thereby emphasizing the importance of modeling auto-contouring SPECT gamma camera motion (with the use of STL volumes) especially for radionuclides with high septal penetration (for e.g. ^{131}I). There could be potential activity underestimation caused by the use of circular motion acquisition thereby impacting the absorbed dose in the dosimetry chain.

STL geometries moreover allow for an easy description of complex phantoms, as an alternative to voxelized phantoms. For instance, a STL-based model of a zebrafish was created from ex-vivo high-resolution micro-CT scans [210]. This phantom has been designed for the MERMAID project, which is aimed to small-fish PET imaging [211]. Figure 10 displays 3D renderings of a PET scanner design and the zebrafish phantom including exemplary photon emissions. Separate STL files were used for different structures (e.g. bones, heart, swim bladder, gills, etc.). These meshes were used as both attenuation and emission phantom. As GATE does not support the distribution of activity within a mesh, Geant4 volumes enclosing the tessellated volumes of interest were created. The activity is distributed within the volume by an acceptance-rejection method. Then, GATE confines the emission of radiation to the respective volume with the *confine* method of its General Particle Source. It should be noted that the acceptance-rejection method can significantly slow down the simulation when the surrounding volumes are much larger than the organs or structures of interest to which the activity should be confined. Care should be thus put in selecting the appropriate size and position of the enclosing volumes.

4.5. Link to third-party reconstruction software

Output from PET, SPECT or Compton camera simulation, either as list mode data or projections images can then be used as input for reconstruction software [52]. Among others, we can cite the following software used to reconstruct 3D images from GATE simulations. STIR (Software for Tomographic Image Reconstruction) [72; 78; 189] was among the first to propose dedicated modules allowing to reconstruction GATE simulated data, both for PET and SPECT, with MLEM and OSEM methods. More recently, the CASToR project [111] (Customizable and Advanced Software for Tomographic Reconstruction) also proposed various reconstruction algorithms for PET and SPECT, with

dedicated tools to use GATE generated data. For SPECT images, the QSPECT software [101; 102; 176] was also employed, in particular to investigate the effect of attenuation correction. Recently in [147; 148], the Reconstruction Toolkit (RTK) [146] was used to provide 4D whole body SPECT reconstruction using image-based breathing signal extraction [148]. The PRESTO toolkit (PET Reconstruction Software Toolkit) [164-166] can also be used with GATE output, such as in [204]. Finally, several Compton Camera reconstruction approaches have been used with GATE data, such as in [81; 126] (MLEM or Origin Ensemble) or in [44; 106] (with conical Radon transform modelling).

4.6. Artificial Intelligence integration

There are several potential interactions between artificial intelligence, deep learning in particular, and Monte Carlo simulations. Within the context of medical imaging, these synergies can be classified in two categories. First, Monte Carlo simulations can produce highly accurate imaging device and patient training datasets for neural networks applied to various signal and image processing tasks. At the detector level, multiple works have been carried out to better determine DOI and/or events positioning within pixelated and continuous monolithic scintillators by using trained neural networks [11; 28; 65; 123; 124; 130; 134; 206; 209]. Training data may be obtained from experimental data acquired with a specific setup or from simulation such as in [206]. In the case of image processing, one can identify tasks specific to the reconstruction and/or the post-processing phase. For example, GATE simulations have been used to provide the input to a U-NET in sinogram space for the derivation of scatter contributions during PET imaging [203]. Deep learning-based scatter correction has been favorably compared with state-of-the art single scatter simulation approaches, independently of the imaging device or anatomical location (tested on lung or pelvis). Similarly, Monte Carlo simulation can generate raw sinograms to training deep-learning networks for PET attenuation correction using MR images [91], or for direct deep learning-based image reconstruction in PET imaging [141]. In terms of image processing, images generated with GATE have been used as part of the training dataset for a functional tumor volume segmentation challenge. Deep learning-based segmentation approaches trained using this dataset showed improved performance compared to state-of-the-art methods [61].

Second, deep learning approaches can be applied to improve Monte Carlo simulation performance, mostly computational efficiency. One example is the simulation-trained neural networks to model detector response. In [160], the authors determined the Angular Response Function (ARF) of a SPECT collimator-detector system with simulation output. The resulting net modelled the probability that a photon is detected, using variance reduction to speed up the simulation. Recently, the concept of Generative Adversarial Networks (GAN) [54] that allow modelling of multidimensional data distributions was proposed to learn a phase space [161] generated by Monte Carlo simulation. Once trained, the generator neural network of the GAN can be used as a very compact source of particles. Similarly, GANs or other more recent variants such as Wasserstein GAN or Deep Convolutional GAN can be applied to generate realistic anthropomorphic models from a few examples of Monte Carlo simulated images with sufficient variability (necessary for training).

Since version 9.0, GATE can be linked to the PyTorch library [133] and methods to interact with the C++ version of this library have been integrated. Trained neural networks can be loaded and used during particle tracking. This integration opens the door to multiple extensions. Indeed, Monte Carlo can generate data ultimately used to train a net or feed the input layer of a net in order to improve the simulation. Note also that deep learning integration is not limited to emission tomography simulation and can be used for dose estimation [55; 92; 100; 128], denoising dose from Monte Carlo simulation both for photon [45; 127; 135] or proton [70; 104], scatter modelling [85; 192], etc. Those studies are still in early stages and further work is needed to better understand the advantages and limitations of mixing deep learning with Monte Carlo approaches. It is a promising field and GATE is ready for it.

5. Conclusion

This article presents an overview of the current status of GATE for emission tomography imaging system simulation, including a large list of systems that have been simulated and, at least partially, validated against experimental data. Recent developments have been described as well and give insight on future improvements in GATE. This comprehensive summary aims at providing an evaluation of the current capabilities and limitations of GATE for imaging systems simulation.

The GATE software has some limitations, partly rooted in the general nature of the Monte Carlo approach, domain-specific problems, and code complexity. First, simulations are generally considered slow, in particular, compared to analytical or semi-analytical methods. Attempts have been made to provide GPU-based acceleration within GATE [12; 13] with acceleration factors from 20 to 400 depending on the simulation type. However, GPU integration in GATE was discontinued due to difficulty to support generic enough graphic card types. Part of this work has been ported to the GGEMS Monte Carlo code [48]. One common alternative solution is to apply parallelization techniques by using multiple CPUs [21]. Users need, however, to pay attention to the time management in the simulation when splitting into parallel jobs, e.g. dead-time or coincidences sorting. Typically, when splitting a PET simulation into several jobs, each job should keep the same activity rate and the whole simulation should be split according to the total simulated acquisition time. Moreover, true coincidences estimation relies on the particle's ID (identification number) provided by the Geant4 kernel in order to ensure the gamma came from the same events. With parallel independent jobs, each job manage his own set of ID. Events ID from one job cannot be mixed with the ones of another job. Tools are provided to adequately split simulations and to merge job's files such as the events IDs are modified and can be compared.

Computation time also limits the use of optical tracking to the simulation of single or pairs of detectors, due to the need for tracking multiple interactions for each optical photon and the high volume of data recorded. As optical Monte Carlo simulation in radiation detectors is increasingly used to study TOF detectors and prompt photons, the complexity of the simulations expands and so do the requirements in terms of computational power. The latest developments in emission tomography are likely to utilize more and more optical tracking capabilities, making this shortcoming a high priority. Another difficulty lies in

the need to precisely know the material and geometrical information of all elements in an imaging system which is often private information that can only be obtained through NDA, preventing publicly share complete imaging models. Another limitation of GATE is that the code source is rather old, more than 15 years, and acknowledges the contributions of numerous volunteers (more than 70 on the current repository that only keeps track of all authors since 2015). Hence, the size and the diversity of the C++ code, more than 350,000 lines of code, makes it relatively hard to maintain. Currently, an effort has been made to modernize the code and adapt a set of engineering techniques e.g. unit tests and continuous integration to improve the code quality. The GATE code typically quickly follows the Geant4 evolutions, thanks to the high responsiveness and support of the Geant4 community. Geant4 toolkit is at the core of simulation in almost every High Energy Physics experiment at CERN [3] and will evolve over the next decade towards various improvements, such as the vectorization technique.

GATE is also used for dosimetry purposes, from optimizing the dose of radiation-based imaging to evaluating absorbed dose distribution during radiation therapy for cancer treatment, in external beam photon and particle therapy, and in internal radionuclide therapy [56; 68; 153; 162]. For example, GATE is one of major contributors to the OpenDose collaboration that aims at providing the community with free resources for Nuclear Medicine dosimetry [25]#. Indeed, the possibility to perform in the same framework imaging and dosimetry studies is important, such as in hadrontherapy monitoring [58; 62; 63; 69] or in the assessment of uncertainties associated with clinical molecular radiotherapy dosimetry [47]††.

Numerous collaborations with the major manufacturers in this field (Philips, GE, Siemens, Spectrum Dynamics, etc.) show that GATE is used not only in academia but also in industry. It might be difficult to make predictions about future GATE development directions because it is largely guided by users' projects and emerging needs. However, we can mention an ongoing trend such as Python binding, which allows performing GATE data analysis using Python scripts, providing access to a large ecosystem of libraries and tools. Moreover, the integration of PyTorch is just at the beginning and may open the doors to developments exploiting Artificial Intelligence methods.

The range of PET and SPECT imaging biomarkers is rapidly expanding for both diagnostic and nuclear theranostic applications [31], and fast timing has now become a key issue for further improving TOF-PET image contrast and reducing radioactive doses injected to the patients [90]. Along the incentive proposed by the 10 ps challenge†, crossing the ambitious 10 ps FWHM CTR frontier which would allow to image a volume virtually without tomographic inversion will necessitate effective, rapid and versatile optical simulation tools to model fast scintillation and prompt photons. In this context, new imaging systems and concepts are being developed to become more quantitative and more cost-effective [185]. The OpenGATE collaboration‡ is committed to follow this evolution providing an

https://opendose.org
†† https://www.dositest.org
† https://the10ps-challenge.org
‡ https://www.opengatecollaboration.org

open-source simulation toolkit dedicated both to research and industry applications in the field of medical imaging, and perhaps numerous other domains utilizing ionizing radiation imaging, such as prompt gamma ray imaging for particle range monitoring in hadrontherapy, X-ray photon counting and neutron imaging for homeland security, or Compton imaging for nuclear decommissioning and nuclear waste management.

Acknowledgments

The Opengate collaboration would like to warmly thanks the Geant4 collaboration for their great support and fruitful discussions.

This work was performed within the framework of the SIRIC LYriCAN Grant INCa-INSERM-DGOS-12563, the LABEX PRIMES (ANR-11-LABX-0063) of Université de Lyon, within the program Investissements d'Avenir (ANR- 11-IDEX-0007) operated by the ANR, and the POPEYE ERA PerMed 2019 project (ANR-19-PERM-0007-04). Optical modeling developments were supported by NIH grants R03 EB020097 and R01 EB027130. STL related work was performed and supported by the MRTDosimetry project§ which is funded by EMPIR program cofinanced by the Participating States and from the European Unions Horizon 2020 research and innovation program. The patient images used were obtained as a part of IAEA Coordinated Research Project (CRP) on Dosimetry in Radiopharmaceutical therapy for personalized patient treatment (E2.30.05). It has also received support by the ENEN+ project that has received funding from the Euratom research and training Work program 2016-2017-1 #75576. The simulations of this work have been performed on the HPC centre CALMIP. The THIDOS project was partially funded by the IN2P3.

References

[1]. Abi Akl M, Bouhali O, Toufique Y, Karp JS, and Vandenberghe S. Monte Carlo sensitivity study of a long axial FOV PET scanner with patient adaptive rings. In 2019 IEEE Nuclear Science Symposium and Medical Imaging Conference (NSS/MIC), pages 1–3, October 2019. doi: 10/ghbjxs.

[2]. Aklan B, Jakoby BW, Watson CC, Braun H, Ritt P, and Quick HH. GATE Monte Carlo simulations for variations of an integrated PET/MR hybrid imaging system based on the Biograph mMR model. Physics in Medicine and Biology, 60(12):4731–4752, June 2015. ISSN 0031-9155. doi: 10/ghck7g. [PubMed: 26040657]

[3]. Albrecht Johannes, Alves Antonio Augusto, Amadio Guilherme, Andronico Giuseppe, Anh-Ky Nguyen, Aphecetche Laurent, Apostolakis John, Asai Makoto, Atzori Luca, Babik Marian, Bagliesi Giuseppe, Bandieramonte Marilena, Banerjee Sunanda, Barisits Martin, Bauerdick Lothar A. T., Belforte Stefano, Benjamin Douglas, Bernius Catrin, Bhimji Wahid, Bianchi Riccardo Maria, Bird Ian, Biscarat Catherine, Blomer Jakob, Bloom Kenneth, Boccali Tommaso, Bockelman Brian, Bold Tomasz, Bonacorsi Daniele, Boveia Antonio, Bozzi Concezio, Bracko Marko, Britton David, Buckley Andy, Buncic Predrag, Calafiura Paolo, Campana Simone, Canal Philippe, Canali Luca, Carlino Gianpaolo, Castro Nuno, Cattaneo Marco, Cerminara Gianluca, Villanueva Javier Cervantes, Chang Philip, Chapman John, Chen Gang, Childers Taylor, Clarke Peter, Clemencic Marco, Cogneras Eric, Coles Jeremy, Collier Ian, Colling David, Corti Gloria, Cosmo Gabriele, Costanzo Davide, Couturier Ben, Cranmer Kyle, Cranshaw Jack, Cristella Leonardo, Crooks David, Crépé-Renaudin Sabine, Currie Robert, Dallmeier-Tiessen Sünje, De Kaushik, De Cian Michel, De Roeck Albert, Peris Antonio Delgado, Derue Frédéric, Di Girolamo Alessandro, Di Guida Salvatore, Dimitrov Gancho, Doglioni Caterina, Dotti Andrea, Duellmann Dirk, Duflot Laurent, Dykstra Dave, Dziedziniewicz-Wojcik Katarzyna, Dziurda Agnieszka, Egede Ulrik, Elmer Peter, Elmsheuser Johannes, Elvira V. Daniel, Eulisse Giulio, Farrell Steven, Ferber Torben, Filipcic Andrej, Fisk Ian, Fitzpatrick Conor, Flix José, Formica Andrea, Forti Alessandra, Franzoni Giovanni, Frost James, Fuess Stu, Gaede Frank, Ganis Gerardo, Gardner Robert, Garonne Vincent, Gellrich Andreas, Genser Krzysztof, George Simon, Geurts Frank, Gheata Andrei, Gheata Mihaela, Giacomini Francesco, Giagu Stefano, Giffels Manuel, Gingrich Douglas, Girone Maria, Gligorov Vladimir V., Glushkov Ivan, Gohn

§ https://mrtdosimetryempir.eu

Wesley, Lopez Jose Benito Gonzalez, Caballero Isidro González, Fernández Juan R. González, Govi Giacomo, Grandi Claudio, Grasland Hadrien, Gray Heather, Grillo Lucia, Guan Wen, Gutsche Oliver, Gyurjyan Vardan, Hanushevsky Andrew, Hariri Farah, Hartmann Thomas, Harvey John, Hauth Thomas, Hegner Benedikt, Heinemann Beate, Heinrich Lukas, Heiss Andreas, Hernández José M., Hildreth Michael, Hodgkinson Mark, Hoeche Stefan, Holzman Burt, Hristov Peter, Huang Xingtao, Ivanchenko Vladimir N., Ivanov Todor, Iven Jan, Jashal Brij, Jayatilaka Bodhitha, Jones Roger, Jouvin Michel, Jun Soon Yung, Kagan Michael, Kalderon Charles William, Kane Meghan, Karavakis Edward, Katz Daniel S., Kcira Dorian, Keeble Oliver, Kersevan Borut Paul, Kirby Michael, Klimentov Alexei, Klute Markus, Komarov Ilya, Konstantinov Dmitri, Koppenburg Patrick, Kowalkowski Jim, Kreczko Luke, Kuhr Thomas, Kutschke Robert, Kuznetsov Valentin, Lampl Walter, Lancon Eric, Lange David, Lassnig Mario, Laycock Paul, Leggett Charles, Letts James, Lewendel Birgit, Li Teng, Lima Guilherme, Linacre Jacob, Linden Tomas, Livny Miron, Presti Giuseppe Lo, Lopienski Sebastian, Love Peter, Lyon Adam, Magini Nicolò, Marshall Zachary L., Martelli Edoardo, Martin-Haugh Stewart, Mato Pere, Mazumdar Kajari, McCauley Thomas, McFayden Josh, McKee Shawn, McNab Andrew, Mehdiyev Rashid, Meinhard Helge, Menasce Dario, Lorenzo Patricia Mendez, Mete Alaettin Serhan, Michelotto Michele, Mitrevski Jovan, Moneta Lorenzo, Morgan Ben, Mount Richard, Moyse Edward, Murray Sean, Nairz Armin, Neubauer Mark S., Norman Andrew, Novaes Sérgio, Novak Mihaly, Oyanguren Arantza, Ozturk Nurcan, Pages Andres Pacheco, Paganini Michela, Pansanel Jerome, Pascuzzi Vincent R., Patrick Glenn, Pearce Alex, Pearson Ben, Pedro Kevin, Perdue Gabriel, Yzquierdo Antonio Perez-Calero, Perrozzi Luca, Petersen Troels, Petric Marko, Petzold Andreas, Piedra Jónatan, Piilonen Leo, Piparo Danilo, Pivarski Jim, Pokorski Witold, Polci Francesco, Potamianos Karolos, Psihas Fernanda, Albert Puig Navarro Günter Quast, Raven Gerhard, Reuter Jürgen, Ribon Alberto, Rinaldi Lorenzo, Ritter Martin, Robinson James, Rodrigues Eduardo, Roiser Stefan, Rousseau David, Roy Gareth, Rybkine Grigori, Sailer Andre, Sakuma Tai, Santana Renato, Sartirana Andrea, Schellman Heidi, Schovancová Jaroslava, Schramm Steven, Schulz Markus, Sciabà Andrea, Seidel Sally, Sekmen Sezen, Serfon Cedric, Severini Horst, Sexton-Kennedy Elizabeth, Seymour Michael, Sgalaberna Davide, Shapoval Illya, Shiers Jamie, Shiu Jing-Ge, Short Hannah, Siroli Gian Piero, Skipsey Sam, Smith Tim, Snyder Scott, Sokoloff Michael D., Spentzouris Panagiotis, Stadie Hartmut, Stark Giordon, Stewart Gordon, Stewart Graeme A., Sánchez Arturo, Sánchez-Hernández Alberto, Taffard Anyes, Tamponi Umberto, Templon Jeff, Tenaglia Giacomo, Tsulaia Vakhtang, Tunnell Christopher, Vaandering Eric, Valassi Andrea, Vallecorsa Sofia, Valsan Liviu, Van Gemmeren Peter, Vernet Renaud, Viren Brett, Vlimant Jean-Roch, Voss Christian, Votava Margaret, Vuosalo Carl, Sierra Carlos Vázquez, Wartel Romain, and The HEP Software Foundation. A Roadmap for HEP Software and Computing R&D for the 2020s. Computing and Software for Big Science, 3(1):7, March 2019. ISSN 2510-2044. doi: 10/ghf3z7.

[4]. Allison J, Amako K, Apostolakis J, Arce P, Asai M, Aso T, Bagli E, Bagulya A, Banerjee S, Barrand G, Beck BR, Bogdanov AG, Brandt D, Brown JMC, Burkhardt H, Canal Ph., Ott D, Chauvie S, Cho K, and Yoshida H. Recent developments in GEANT4. Nuclear Instruments and Methods in Physics Research Section A: Accelerators, Spectrometers, Detectors and Associated Equipment, 835:186–225, 2016.

[5]. Ariño-Estrada Gerard, Roncali Emilie, Selfridge Aaron R, Du Junwei, Glodo Jaroslaw, Shah Kanai S., and Cherry Simon R.. Study of Cerenkov Light Emission in the Semiconductors TlBr and TlCl for TOF-PET. IEEE Transactions on Radiation and Plasma Medical Sciences, pages 1–1, 2020. ISSN 2469-7303. doi: 10/ghfdbp.

[6]. Assie K, Gardin I, Vera P, and Buvat I. Validation of gate Monte Carlo simulations for indium 111 imaging. In IEEE Symposium Conference Record Nuclear Science 2004., volume 7, pages 4023–4027, October 2004. doi: 10/cdzgb8.

[7]. Assié Karine, Breton Vincent, Buvat Irène, Comtat Claude, Jan Sébastien, Krieguer Magalie, Lazaro Delphine, Morel Christian, Rey Martin, Santin Giovanni, Simon Luc, Staelens Steven, Strul Daniel, Vieira Jean-Marc, and Van de Walle Rik. Monte Carlo simulation in PET and SPECT instrumentation using GATE. Nuclear Instruments and Methods in Physics Research Section A: Accelerators, Spectrometers, Detectors and Associated Equipment, 527(1):180–189, July 2004. ISSN 0168-9002. doi: 10/cs2td3.

[8]. Autret Damien, Bitar Abdelkader, Ferrer Ludovic, Lisbona Albert, and Bardiès Manuel. Monte Carlo modeling of gamma cameras for I-131 imaging in targeted radiotherapy. Cancer biotherapy & radiopharmaceuticals, 20(1):77–84, February 2005. ISSN 1084-9785. doi: 10.1089/cbr.2005.20.77. [PubMed: 15778585]

[9]. Bastiaannet Remco, Kappadath S. Cheenu, Kunnen Britt, Braat Arthur J. A. T., Lam Marnix G. E. H., and de Jong Hugo W. A. M.. The physics of radioembolization. EJNMMI Physics, 5, November 2018. ISSN 2197-7364. doi: 10/gfmtmb.

[10]. Bataille F, Comtat C, Jan S, and Trebossen R. Monte Carlo simulation for the ECAT HRRT using GATE. In IEEE Symposium Conference Record Nuclear Science 2004., volume 4, pages 2570–2574 Vol. 4, October 2004. doi: 10/c2gn9c.

[11]. Berg Eric and Cherry Simon R.. Using convolutional neural networks to estimate time-of-flight from PET detector waveforms. Physics in Medicine and Biology, 63(2):02LT01, January 2018. ISSN 1361-6560. doi: 10/ghc3vv.

[12]. Bert J, Perez-Ponce H, Jan S, El Bitar Z, Gueth P, Cuplov V, Chekatt H, Benoit D, Sarrut D, Boursier Y, Brasse D, Buvat I, Morel C, and Visvikis D. Hybrid GATE: A GPU/CPU implementation for imaging and therapy applications. In 2012 IEEE Nuclear Science Symposium and Medical Imaging Conference Record (NSS/MIC), pages 2247–2250, October 2012. doi: 10/ghn45p.

[13]. Bert Julien, Perez-Ponce Hector, El Bitar Ziad, Jan Sébastien, Boursier Yannick, Vintache Damien, Bonissent Alain, Morel Christian, Brasse David, and Visvikis Dimitris. Geant4-based Monte Carlo simulations on GPU for medical applications. Physics in Medicine and Biology, 58(16):5593–5611, August 2013. ISSN 0031-9155, 1361-6560. doi: 10/gf9266. [PubMed: 23892709]

[14]. Boisson F, Bekaert V, El Bitar Z, Wurtz J, Steibel J, and Brasse D. Characterization of a rotating slat collimator system dedicated to small animal imaging. Physics in Medicine and Biology, 56(5):1471–1485, February 2011. ISSN 0031-9155. doi: 10/bmkr7m. [PubMed: 21321386]

[15]. Brun Rene and Rademakers Fons. ROOT — An object oriented data analysis framework. Nuclear Instruments and Methods in Physics Research Section A: Accelerators, Spectrometers, Detectors and Associated Equipment, 389(1-2):81–86, April 1997. ISSN 01689002. doi: 10/cxnq7s.

[16]. Brunner SE and Schaart DR. BGO as a hybrid scintillator / Cherenkov radiator for cost-effective time-of-flight PET. Physics in Medicine and Biology, 62(11):4421–4439, June 2017. ISSN 1361-6560. doi: 10/ghfdbh. [PubMed: 28358722]

[17]. Bruyndonckx Peter, Lemaître Cedric, Schaart Dennis, Maas Marnix, van der Laan D. J. (jan), Krieguer Magalie, Devroede Olivier, and Tavernier Stefaan. Towards a continuous crystal APD-based PET detector design. Nuclear Instruments and Methods in Physics Research Section A: Accelerators, Spectrometers, Detectors and Associated Equipment, 571(1):182–186, February 2007. ISSN 0168-9002. doi: 10/ffg84d.

[18]. Buvat I and Lazaro D. Monte Carlo simulations in emission tomography and GATE: An overview. Nucl. Instr. Meth. Phys. Res, 569:323–329, 2006.

[19]. Cabello Jorge and Ziegler Sibylle I.. Advances in PET/MR instrumentation and image reconstruction. The British Journal of Radiology, 91(1081):20160363, January 2018. ISSN 1748-880X. doi: 10/gct3qk. [PubMed: 27376170]

[20]. Cajgfinger Thomas, Rit Simon, Létang Jean Michel, Halty Adrien, and Sarrut David. Fixed forced detection for fast SPECT Monte-Carlo simulation. Physics in Medicine & Biology, 63(5):055011, 2018. doi: 10.1088/1361-6560/aa9e32. [PubMed: 29185992]

[21]. Camarasu-Pop Sorina, Glatard Tristan, Mościcki Jakub T., Benoit-Cattin Hugues, and Sarrut David. Dynamic Partitioning of GATE Monte-Carlo Simulations on EGEE. Journal of Grid Computing, 8(2):241–259, June 2010. ISSN 1570-7873, 1572-9184. doi: 10/ftjtgf.

[22]. Canot C, Alokhina M, Abbon P, Bard JP, Tauzin G, Yvon D, and Sharyy V. Development of the fast and efficient gamma detector using Cherenkov light for TOF-PET. Journal of Instrumentation, 12(12):C12029–C12029, December 2017. ISSN 1748-0221. doi: 10/gh58pv.

[23]. Carlier Thomas, Moisan Maxime, Ferrer Ludovic, Kraeber-Bodere Francoise, Barbet Jacques, and Bardies Manuel. Validation of a GATE model of the Siemens Symbia system for 99mTc, 111In and 131I acquisitions. Journal of Nuclear Medicine, 49(supplement 1):405P–405P, May 2008. ISSN 0161-5505, 2159-662X.

[24]. Cates Joshua W., Gundacker Stefan, Auffray Etiennette, Lecoq Paul, and Levin Craig S.. Improved single photon time resolution for analog SiPMs with front end readout that reduces influence of electronic noise. Physics in Medicine & Biology, 63(18):185022, September 2018. ISSN 0031-9155. doi: 10/ghfdbk. [PubMed: 30129562]

[25]. Chauvin Maxime, Borys Damian, Botta Francesca, Bzowski Pawel, Dabin Jérémie, Denis-Bacelar Ana M, Desbrée Aurélie, Falzone Nadia, Lee Boon Quand, Mairiani Andrea, Malaroda Alessandra, Mathieu Gilles, McKay Erin, Mora-Ramirez Erick, Robinson Andrew P, Sarrut David, Struelens Lara, Gil Alex Vergara, and Bardiès Manuel. OpenDose: Open access resources for nuclear medicine dosimetry. Journal of Nuclear Medicine, page jnumed.119.240366, March 2020. ISSN 0161-5505, 2159-662X. doi: 10/ggw5t7.

[26]. Cherry Simon R., Sorenson James A., and Phelps Michael E., editors. Physics in Nuclear Medicine. W.B. Saunders, Philadelphia, January 2012. ISBN 978-1-4160-5198-5. doi: 10.1016/B978-1-4160-5198-5.00033-2.

[27]. Chung Yong Hyun, Choi Yong, Cho Gyuseong, Choe Yearn Seong, Lee Kyung-Han, and Kim Byung-Tae. Optimization of dual Layer phoswich detector consisting of LSO and LuYAP for small animal PET. IEEE Transactions on Nuclear Science, 52(1):217–221, February 2005. ISSN 1558-1578. doi: 10/dc5f62.

[28]. Conde P, Iborra A, González AJ, Hernández L, Bellido P, Moliner L, Rigla JP, Rodríguez-Álvarez MJ, Sánchez F, Seimetz M, Soriano A, Vidal LF, and Benlloch JM. Determination of the Interaction Position of Gamma Photons in Monolithic Scintillators Using Neural Network Fitting. IEEE Transactions on Nuclear Science, 63(1):30–36, February 2016. ISSN 1558-1578. doi: 10/f8d35g.

[29]. Conti Maurizio and Bendriem Bernard. The new opportunities for high time resolution clinical TOF PET. Clinical and Translational Imaging, 7(2):139–147, April 2019. ISSN 2281-7565. doi: 10/ghdrqx.

[30]. Costa GCA, Bonifácio DAB, Sarrut D, Cajgfinger T, and Bardiès M. Optimization of GATE simulations for whole-body planar scintigraphic acquisitions using the XCAT male phantom with 177Lu-DOTATATE biokinetics in a Siemens Symbia T2. Physica Medica, 42:292–297, October 2017. ISSN 1120-1797. doi: 10/gf6846. [PubMed: 28736285]

[31]. Czernin Johannes, Sonni Ida, Razmaria Aria, and Calais Jeremie. The Future of Nuclear Medicine as an Independent Specialty. Journal of Nuclear Medicine, 60(Supplement 2):3S–12S, September 2019. ISSN 0161-5505, 2159-662X. doi: 10/ghf3fh. [PubMed: 31481589]

[32]. Decuyper Milan, Stockhoff Mariele, and Van Holen Roel. Deep learning for positioning of gamma interactions in monolithic PET detectors. In 2019 IEEE Nuclear Science Symposium and Medical Imaging Conference (NSS/MIC), Abstracts, 2019.

[33]. Decuyper Milan, Stockhoff Mariele, Vandenberghe Stefaan, and Van Holen Roel. Artificial neural networks for positioning of gamma interactions in monolithic PET detectors. Physics in Medicine & Biology, 66(7):075001, March 2021. ISSN 0031-9155. doi: 10.1088/1361-6560/abebfc.

[34]. Degenhardt Carsten, Prescher Gordian, Frach Thomas, Thon Andreas, de Gruyter Rik, Schmitz Anja, and Ballizany Rob. The digital Silicon Photomultiplier — A novel sensor for the detection of scintillation light. In 2009 IEEE Nuclear Science Symposium Conference Record (NSS/MIC), pages 2383–2386, October 2009. doi: 10/cf8whq.

[35]. Del Guerra Alberto, Ahmad Salleh, Avram Mihai, Belcari Nicola, Berneking Arne, Biagi Laura, Bisogni Maria Giuseppina, Brandl Felix, Cabello Jorge, Camarlinghi Niccolò, Cerello Piergiorgio, Choi Chang-Hoon, Coli Silvia, Colpo Sabrina, Fleury Julien, Gagliardi Vito, Giraudo Giuseppe, Heekeren Karsten, Kawohl Wolfram, Kostou Theodora, Lefaucheur Jean-Luc, Lerche Christoph, Loudos George, Morrocchi Matteo, Muller Julien, Mustafa Mona, Neuner Irene, Papadimitroulas Panagiotis, Pennazio Francesco, Rajkumar Ravichandran, Brambilla Cláudia Régio, Rivoire Julien, Kops Elena Rota, Scheins Jürgen, Schimpf Rémy, Shah N. Jon, Sorg Christian, Sportelli Giancarlo, Tosetti Michela, Trinchero Riccardo, Wyss Christine, Ziegler Sibylle and TRIMAGE Consortium. TRIMAGE: A dedicated trimodality (PET/MR/EEG) imaging tool for schizophrenia. European Psychiatry: The Journal of the Association of European Psychiatrists, 50:7–20, April 2018. ISSN 1778-3585. doi: 10/gdf7hn. [PubMed: 29358016]

[36]. Descourt P, Carlier T, Du Y, Song X, Buvat I, Frey EC, Bardies M, Tsui BMW, Visvikis D. Implementation of angular response function modeling in SPECT simulations with GATE. Physics in Medicine and Biology, 55(9):N253–N266, May 2009. ISSN 0031-9155, 1361-6560. doi: 10/bkcct9.

[37]. Dietze Martijn M. A., van der Velden Sandra, Lam Marnix G. E. H., Viergever Max A., and de Jong Hugo W. A. M.. Fast quantitative reconstruction with focusing collimators for liver SPECT. EJNMMI Physics, 5, December 2018. ISSN 2197-7364. doi: 10/ghn45t.

[38]. Emami Azadeh, Ghafarian Pardis, Ghadiri Hossien, Geramifar Parham, and Ay Mohammad Reza. Validation and evaluation of a GATE model for MAMMI PET scanner. Iranian Journal of Nuclear Medicine, 28(1):33–38, January 2020. ISSN 1681-2824.

[39]. Etxebeste A, Dauvergne D, Fontana M, Létang JM, Llosá G, Munoz E, Oliver JF, Testa É, and Sarrut D. CCMod: A GATE module for Compton camera imaging simulation. Physics in Medicine and Biology, 65(5):055004, February 2020. ISSN 1361-6560. doi: 10/ggw5t8. [PubMed: 31869822]

[40]. Etxebeste Ane, Barrio John, Muñoz Enrique, Oliver Josep F., Solaz Carles, and Llosá Gabriela. 3D position determination in monolithic crystals coupled to SiPMs for PET. Physics in Medicine and Biology, 61(10):3914–3934, April 2016. ISSN 0031-9155. doi: 10.1088/0031-9155/61/10/3914. [PubMed: 27119737]

[41]. Everett DB, Fleming JS, Todd RW, and Nightingale JM. Gamma-radiation imaging system based on the Compton effect. Proceedings of the Institution of Electrical Engineers, 124(11):995–1000, November 1977. ISSN 2053-7891. doi: 10/d9ggh2.

[42]. Fanchon Louise. Autoradiographic Quantitative d'échantillons Prélevés Par Biopsie Guidée Par TEP/TDM : Méthode et Applications Cliniques. These de doctorat, Brest, March 2016.

[43]. Fanchon Louise M., Dogan Snjezana, Moreira Andre L., Carlin Sean A., Schmidtlein C. Ross, Yorke Ellen, Apte Aditya P., Burger Irene A., Durack Jeremy C., Erinjeri Joseph P., Maybody Majid, Schöder Heiko, Siegelbaum Robert H., Sofocleous Constantinos T., Deasy Joseph O., Solomon Stephen B., Humm John L., Kirov Assen S.. Feasibility of in situ, high-resolution correlation of tracer uptake with histopathology by quantitative autoradiography of biopsy specimens obtained under 18F-FDG PET/CT guidance. Journal of Nuclear Medicine: Official Publication, Society of Nuclear Medicine, 56(4):538–544, April 2015. ISSN 1535-5667. doi: 10/f66r26. [PubMed: 25722446]

[44]. Feng Yuemeng, Etxebeste Ane, Sarrut David, Létang Jean Michel, and Maxim Voichiţa. 3-D Reconstruction Benchmark of a Compton Camera Against a Parallel-Hole Gamma Camera on Ideal Data. IEEE Transactions on Radiation and Plasma Medical Sciences, 4(4):479–488, July 2020. ISSN 2469-7303. doi: 10/ggw5vc.

[45]. Fornander Hannes. Denoising Monte Carlo Dose Calculations Using a Deep Neural Network. PhD thesis, KTH Royal Institute Of Technology School of Electrical Engineering and Computer Science, 2019.

[46]. Frach Thomas, Prescher Gordian, Degenhardt Carsten, de Gruyter Rik, Schmitz Anja, and Ballizany Rob. The digital silicon photomultiplier — Principle of operation and intrinsic detector performance. In 2009 IEEE Nuclear Science Symposium Conference Record (NSS/MIC), pages 1959–1965, October 2009. doi: 10/dpgzpq.

[47]. Garcia Marie-Paule, Villoing Daphnée, McKay Erin, Ferrer Ludovic, Cremonesi Marta, Botta Francesca, Ferrari Mahila, and Bardiès Manuel. TestDose: A nuclear medicine software based on Monte Carlo modeling for generating gamma camera acquisitions and dosimetry. Med Phys, 42(12):6885–6894, December 2015. doi: 10.1118/1.4934828. [PubMed: 26632045]

[48]. Garcia Marie-Paule, Bert Julien, Benoit Didier, Bardiès Manuel, and Visvikis Dimitris. Accelerated GPU based SPECT Monte Carlo simulations. Phys Med Biol, 61(11):4001–4018, June 2016. doi: 10.1088/0031-9155/61/11/4001. [PubMed: 27163656]

[49]. Georgiou Maria, Fysikopoulos Eleftherios, Mikropoulos Konstantinos, Fragogeorgi Eirini, and Loudos George. Characterization of "γ-Eye": A Low-Cost Benchtop Mouse-Sized Gamma Camera for Dynamic and Static Imaging Studies. Molecular Imaging and Biology, 19(3):398–407, June 2017. ISSN 1860-2002. doi: 10/ghdrdn. [PubMed: 27730469]

[50]. Geramifar P, Ay MR, Shamsaie Zafarghandi M, Sarkar S, Loudos G, and Rahmim A. Investigation of time-of-flight benefits in an LYSO-based PET/CT scanner: A Monte Carlo

study using GATE. Nuclear Instruments and Methods in Physics Research Section A: Accelerators, Spectrometers, Detectors and Associated Equipment, 641(1):121–127, June 2011. ISSN 0168-9002. doi: 10/bn46nv.

[51]. Geramifar Parham, Ay Mohammad Reza, Zafarghandi Mojtaba Shamsaie, Loudos George, and Rahmim Arman. Performance comparison of four commercial GE discovery PET/CT scanners: A monte carlo study using GATE. Iranian Journal of Nuclear Medicine, 17(2):26–33, December 2009. ISSN 1681-2824.

[52]. Gillam John E. and Rafecas Magdalena. Monte-Carlo simulations and image reconstruction for novel imaging scenarios in emission tomography. Nuclear Instruments and Methods in Physics Research Section A: Accelerators, Spectrometers, Detectors and Associated Equipment, 809:76–88, February 2016. ISSN 01689002. doi: 10/f74zkc.

[53]. Gonias P, Bertsekas N, Karakatsanis N, Saatsakis G, Gaitanis A, Nikolopoulos D, Loudos G, Papaspyrou L, Sakellios N, Tsantilas X, Daskalakis A, Liaparinos P, Nikita K, Louizi A, Cavouras D, Kandarakis I, and Panayiotakis GS. Validation of a GATE model for the simulation of the Siemens biograph™ 6 PET scanner. Nuclear Instruments and Methods in Physics Research Section A: Accelerators, Spectrometers, Detectors and Associated Equipment, 571(1):263–266, February 2007. ISSN 0168-9002. doi: 10/c836t6.

[54]. Goodfellow Ian, Pouget-Abadie Jean, Mirza Mehdi, Xu Bing, Warde-Farley David, Ozair Sherjil, Courville Aaron, and Bengio Yoshua. Generative adversarial nets. In Advances in Neural Information Processing Systems, volume 2, pages 2672–2680, 2014.

[55]. Götz Theresa Ida, Schmidkonz Christian, Chen Shuqing, Al-Baddai Saad, Kuwert Torsten, and Lang Elmar W.. A deep learning approach to radiation dose estimation. Physics in Medicine and Biology, December 2019. ISSN 1361-6560. doi: 10/ggjtbn.

[56]. Grevillot L, Boersma DJ, Fuchs H, Aitkenhead A, Elia A, Bolsa M, Winterhalter C, Vidal M, Jan S, Pietrzyk U, Maigne L, and Sarrut D. GATE-RTion: A GATE/Geant4 release for clinical applications in scanned ion beam therapy. Medical Physics, n/a(n/a), 2020. ISSN 2473-4209. doi: 10/ghbjz6.

[57]. Groiselle CJ, Kudrolli HA, and Glick SJ. Monte-Carlo simulation of the photodetection systems prototype PET scanner using GATE: A validation study. In IEEE Symposium Conference Record Nuclear Science 2004., volume 5, pages 3130–3132, October 2004. doi: 10/ds7rvf.

[58]. Gueth P, Dauvergne D, Freud N, Létang JM, Ray C, Testa E, and Sarrut D. Machine learning-based patient specific prompt-gamma dose monitoring in proton therapy. Physics in Medicine & Biology, 58(13):4563–4577, July 2013. doi: 10.1088/0031-9155/58/13/4563. [PubMed: 23771015]

[59]. Harris Charles R., Millman K. Jarrod, van der Walt Stéfan J., Gommers Ralf, Virtanen Pauli, Cournapeau David, Wieser Eric, Taylor Julian, Berg Sebastian, Smith Nathaniel J., Kern Robert, Picus Matti, Hoyer Stephan, van Kerkwijk Marten H., Brett Matthew, Haldane Allan, Del Río Jaime Fernández, Wiebe Mark, Peterson Pearu, Gérard-Marchant Pierre, Sheppard Kevin, Reddy Tyler, Weckesser Warren, Abbasi Hameer, Gohlke Christoph, Oliphant Travis E.. Array programming with NumPy. Nature, 585(7825):357–362, September 2020. ISSN 1476-4687. doi: 10/ghbzf2. [PubMed: 32939066]

[60]. Hartl Alexander, Shakir Dzhoshkun I., Lasser Tobias, Ziegler Sibylle I., and Navab Nassir. Detection models for freehand SPECT reconstruction. Physics in Medicine and Biology, 60(3):1031–1046, February 2015. ISSN 1361-6560. doi: 10/ghn45w. [PubMed: 25585618]

[61]. Hatt Mathieu, Laurent Baptiste, Ouahabi Anouar, Fayad Hadi, Tan Shan, Li Laquan, Lu Wei, Jaouen Vincent, Tauber Clovis, Czakon Jakub, Drapejkowski Filip, Dyrka Witold, Camarasu-Pop Sorina, Cervenansky Frédéric, Girard Pascal, Glatard Tristan, Kain Michael, Yao Yao, Barillot Christian, Kirov Assen, and Visvikis Dimitris. The first MICCAI challenge on PET tumor segmentation. Medical Image Analysis, 44:177–195, February 2018. ISSN 1361-8423. doi: 10/gc22mx. [PubMed: 29268169]

[62]. Hilaire Estelle, Sarrut David, Peyrin Françoise, and Maxim Voichiţa. Proton therapy monitoring by Compton imaging: Influence of the large energy spectrum of the prompt-γ radiation. Physics in Medicine & Biology, 61(8):3127, April 2016. ISSN 1361-6560. doi: 10.1088/0031-9155/61/8/3127. [PubMed: 27008459]

[63]. Huisman Brent FB, Létang Jean Michel, Testa É, and Sarrut David. Accelerated prompt gamma estimation for clinical proton therapy simulations. Physics in Medicine & Biology, 61(21):7725, November 2016. ISSN 1361-6560. doi: 10.1088/0031-9155/61/21/7725. [PubMed: 27740939]

[64]. Hunter John D.. Matplotlib: A 2D Graphics Environment. Computing in Science Engineering, 9(3):90–95, May 2007. ISSN 1558-366X. doi: 10/drbjhg.

[65]. Iborra A, González AJ, González-Montoro A, Bousse A, and Visvikis D. Ensemble of neural networks for 3D position estimation in monolithic PET detectors. Physics in Medicine & Biology, 64(19):195010, October 2019. ISSN 0031-9155. doi: 10/ghbjxg. [PubMed: 31416053]

[66]. Jan S, Santin G, Strul D, Staelens S, Assié K, Autret D, Avner S, Barbier R, Bardiès M, Bloomfield PM, Brasse D, Breton V, Bruyndonckx P, Buvat I, Chatziioannou AF, Choi Y, Chung YH, Comtat C, Donnarieix D, Ferrer L, Glick SJ, Groiselle CJ, Guez D, Honore P-F, Kerhoas-Cavata S, Kirov AS, Kohli V, Koole M, Krieguer M, van der Laan DJ, Lamare F, Largeron G, Lartizien C, Lazaro D, Maas MC, Maigne L, Mayet F, Melot F, Merheb C, Pennacchio E, Perez J, Pietrzyk U, Rannou FR, Rey M, Schaart DR, Schmidtlein CR, Simon L, Song TY, Vieira J-M, Visvikis D, Van de Walle R, Wieërs E, Morel C. GATE: A simulation toolkit for PET and SPECT. Physics in Medicine and Biology, 49(19):4543–4561, October 2004. ISSN 0031-9155, 1361-6560. doi: 10/dz8473. [PubMed: 15552416]

[67]. Jan S, Comtat C, Strul D, Santin G, and Trebossen R. Monte Carlo Simulation for the ECAT EXACT HR+ system using GATE. IEEE Transactions on Nuclear Science, 52(3):627–633, June 2005. ISSN 1558-1578. doi: 10/fjxgxq.

[68]. Jan S, Benoit D, Becheva E, Carlier T, Cassol F, Descourt P, Frisson T, Grevillot L, Guigues L, Maigne L, Morel C, Perrot Y, Rehfeld N, Sarrut D, Schaart DR, Stute S, Pietrzyk U, Visvikis D, Zahra N, and Buvat I. GATE V6: A major enhancement of the GATE simulation platform enabling modelling of CT and radiotherapy. Phys Med Biol, 56(4):881–901, February 2011. doi: 10.1088/0031-9155/56/4/001. [PubMed: 21248393]

[69]. Jan Sebastien, Frisson Thibault, and Sarrut David. GATE simulation of 12C hadrontherapy treatment combined with a PET imaging system for dose monitoring: A feasibility study. IEEE TRANSACTIONS ON NUCLEAR SCIENCE, page 7, 2012.

[70]. Javaid Umair, Souris Kevin, Dasnoy Damien, Huang Sheng, and Lee John A.. Mitigating inherent noise in Monte Carlo dose distributions using dilated U-Net. Medical Physics, 46(12):5790–5798, 2019. ISSN 2473-4209. doi: 10/ghbjz8. [PubMed: 31600829]

[71]. Kamińska D, Gajos A, Czerwiński E, Alfs D, Bednarski T, Białas P, Curceanu C, Dulski K, Głowacz B, Gupta-Sharma N, Gorgol M, Hiesmayr BC, Jasińska B, Korcyl G, Kowalski P, Krzemień W, Krawczyk N, Kubicz E, Mohammed M, Niedźwiecki Sz., Pawlik-Niedźwiecka M, Raczyński L, Rudy Z, Silarski M, Wieczorek A, Wiślicki W, Zgardzińska B, Zieliński M, Moskal P. A feasibility study of ortho-positronium decays measurement with the J-PET scanner based on plastic scintillators. The European Physical Journal C, 76(8):445, August 2016. ISSN 1434-6052. doi: 10/ghdrqf. [PubMed: 27547122]

[72]. Kang Han Gyu, Tashima Hideaki, Hong Seong Jong, and Yamaya Taiga. Optimization of a High Resolution Small Animal SPECT System using GATE and STIR Software. In 2018 IEEE Nuclear Science Symposium and Medical Imaging Conference Proceedings (NSS/MIC), pages 1–3, November 2018. doi: 10/ghbjxm.

[73]. Karakatsanis N, Sakellios N, Tsantilas NX, Dikaios N, Tsoumpas C, Lazaro D, Loudos G, Schmidtlein CR, Louizi K, Valais J, Nikolopoulos D, Malamitsi J, Kandarakis J, and Nikita K. Comparative evaluation of two commercial PET scanners, ECAT EXACT HR+ and Biograph 2, using GATE. Nuclear Instruments and Methods in Physics Research Section A: Accelerators, Spectrometers, Detectors and Associated Equipment, 569(2):368–372, December 2006. ISSN 0168-9002. doi: 10/bqtxfq.

[74]. Kayal Gunjan, Chauvin Maxime, Mora-Ramirez Erick, Clayton Naomi, Gil Alex Vergara, Tran-Gia Johannes, Lassmann Michael, Struelens Lara, and Bardies Manuel. Modeling SPECT auto-contouring acquisition for 177Lu & 131I Molecular Radiotherapy using new developments in Geant4/GATE. Submitted, 2020.

[75]. Kayal Gunjan, Chauvin Maxime, Mora-Ramirez Erick, Struelens Lara, and Bardies Manuel. Implementation of SPECT auto-contouring detector motion in GATE Monte Carlo simulation for 177Lu and 131I Molecular Radiotherapy (MRT) dosimetry. In European Association of

Nuclear Medicine (EANM) Annual Congress, volume 47 of 1–753, Vienna, 2020. doi: 10.1007/s00259-020-04988-4.

[76]. Kayal Gunjan, Chauvin Maxime, Gil Alex Vergara, Clayton Naomi, Struelens Lara, and Bardies Manuel. Generation of realistic SPECT/CT images for 177Lu dosimetry in Molecular Radiotherapy (MRT) based on Monte Carlo simulation with GATE. In European Association of Nuclear Medicine (EANM) Annual Congress, volume 47 of 1–753, Vienna, 2020. doi: 10.1007/s00259-020-04988-4.

[77]. Kayal Gunjan, Chauvin Maxime, Gil Alex Vergara, Clayton Naomi, Ferrer Ludovic, Moalosi Tumelo, Knoll Peter, Struelens Lara, and Bardies Manuel. Generation of clinical 177Lu SPECT/CT images based on Monte Carlo simulation with GATE. Physica Medica, 2021.

[78]. Khateri Parisa, Fischer Jannis, Lustermann Werner, Tsoumpas Charalampos, and Dissertori Günther. Implementation of cylindrical PET scanners with block detector geometry in STIR. EJNMMI Physics, 6(1):15, December 2019. ISSN 2197-7364. doi: 10/gf685k. [PubMed: 31359303]

[79]. Kirov Assen S., Fanchon Louise M., Seiter Daniel, Czmielewski Christian, Russell James, Dogan Snjezana, Carlin Sean, Pinker-Domenig Katja, Yorke Ellen, Schmidtlein C. Ross, Boyko Vitaly, Fujisawa Sho, Manova-Todorova Katia, Zanzonico Pat, Dauer Lawrence, Deasy Joseph O., Humm John L., Solomon Stephen. Technical Note: Scintillation well counters and particle counting digital autoradiography devices can be used to detect activities associated with genomic profiling adequacy of biopsy specimens obtained after a low activity 18 F-FDG injection. Medical Physics, 45(5):2179–2185, May 2018. ISSN 2473-4209. doi: 10/gc7tz3. [PubMed: 29480927]

[80]. Kochebina Olga, Jan Sébastien, Stute Simon, Sharyy Viatcheslav, Verrecchia Patrice, Mancardi Xavier, and Yvon Dominique. Performance Estimation for the High Resolution CaLIPSO Brain PET Scanner: A Simulation Study. IEEE Transactions on Radiation and Plasma Medical Sciences, 3(3):363–370, May 2019. ISSN 2469-7303. doi: 10/ghbjz2.

[81]. Kohlhase Nadja, Wegener Tilman, Schaar Moritz, Bolke Andreas, Etxebeste Ane, Sarrut David, and Rafecas Magdalena. Capability of MLEM and OE to Detect Range Shifts With a Compton Camera in Particle Therapy. IEEE Transactions on Radiation and Plasma Medical Sciences, 4(2):233–242, March 2020. ISSN 2469-7311, 2469-7303. doi: 10/gf82xt.

[82]. Kowalski P, Wiślicki W, Shopa RY, Raczyński L, Klimaszewski K, Curcenau C, Czerwiński E, Dulski K, Gajos A, Gorgol M, Gupta-Sharma N, Hiesmayr B, Jasińska B, Kapłon Ł, Kisielewska-Kamińska D, Korcyl G, Kozik T, Krzemień W, Kubicz E, Mohammed M, Niedźwiecki S, Pałka M, Pawlik-Niedźwiecka M, Raj J, Rakoczy K, Rudy Z, Sharma S, Shivani S, Silarski M, Skurzok M, Zgardzińska B, Zieliński M, Moskal P. Estimating the NEMA characteristics of the J-PET tomograph using the GATE package. Physics in Medicine & Biology, 63(16):165008, August 2018. ISSN 1361-6560. doi: 10/ghbjxz. [PubMed: 29992906]

[83]. Kwon Sun Il, Gola Alberto, Ferri Alessandro, Piemonte Claudio, and Cherry Simon R.. Bismuth germanate coupled to near ultraviolet silicon photomultipliers for time-of-flight PET. Physics in Medicine and Biology, 61(18):L38–L47, September 2016. ISSN 1361-6560. doi: 10/ghfdbj. [PubMed: 27589153]

[84]. Kwon Sun Il, Roncali Emilie, Gola Alberto, Paternoster Giovanni, Piemonte Claudio, and Cherry Simon R.. Dual-ended readout of bismuth germanate to improve timing resolution in time-of-flight PET. Physics in Medicine & Biology, 64(10):105007, May 2019. ISSN 0031-9155. doi: 10/ghfdbq. [PubMed: 30978713]

[85]. Lalonde Arthur, Winey Brian A., Verburg Joost M., Paganetti Harald, and Sharp Gregory C.. Evaluation of CBCT scatter correction using deep convolutional neural networks for head and neck adaptive proton therapy. Physics in Medicine & Biology, 2020. ISSN 0031-9155. doi: 10.1088/1361-6560/ab9fcb.

[86]. Lamare F, Turzo A, Bizais Y, Cheze Le Rest C, and Visvikis D. Validation of a Monte Carlo simulation of the Philips Allegro/GEMINI PET systems using GATE. Physics in Medicine and Biology, 51(4):943–962, February 2006. ISSN 0031-9155. doi: 10/bs27d8. [PubMed: 16467589]

[87]. Lazaro D, Buvat I, Loudos G, Strul D, Santin G, Giokaris N, Donnarieix D, Maigne L, Spanoudaki V, Styliaris S, Staelens S, and Breton V. Validation of the GATE Monte Carlo simulation platform for modelling a CsI(Tl) scintillation camera dedicated to small-animal

imaging. Physics in Medicine and Biology, 49(2):271–285, January 2004. ISSN 0031-9155. doi: 10/c33m9f. [PubMed: 15083671]

[88]. Lecoq P. New Approaches to Improve Timing Resolution in Scintillators. IEEE Transactions on Nuclear Science, 59(5):2313–2318, October 2012. ISSN 1558-1578. doi: 10/f4cv8b.

[89]. Lecoq P. Pushing the Limits in Time-of-Flight PET Imaging. IEEE Transactions on Radiation and Plasma Medical Sciences, 1(6):473–485, November 2017. ISSN 2469-7303. doi: 10/ghfdbn.

[90]. Lecoq Paul, Morel Christian, Prior John O., Visvikis Dimitris, Gundacker Stefan, Auffray Etiennette, Križan Peter, Turtos Rosana Martinez, Thers Dominique, Charbon Edoardo, Varela Joao, de La Taille Christophe, Rivetti Angelo, Breton Dominique, Pratte Jean-François, Nuyts Johan, Surti Suleman, Vandenberghe Stefaan, Marsden Paul, Parodi Katia, Benlloch Jose Maria, Benoit Mathieu. Roadmap toward the 10 ps time-of-flight PET challenge. Physics in Medicine & Biology, 65(21):21RM01, October 2020. ISSN 0031-9155. doi: 10/ghkfw8.

[91]. Lee JS. A Review of Deep Learning-Based Approaches for Attenuation Correction in Positron Emission Tomography. IEEE Transactions on Radiation and Plasma Medical Sciences, pages 1–1, 2020. ISSN 2469-7303. doi: 10/ghkdh7.

[92]. Lee Min Sun, Hwang Donghwi, Kim Joong Hyun, and Lee Jae Sung. Deep-dose: A voxel dose estimation method using deep convolutional neural network for personalized internal dosimetry. Scientific Reports, 9(1):10308, December 2019. ISSN 2045-2322. doi: 10/gf684s. [PubMed: 31311963]

[93]. Lee Sanghyeb, Gregor Jens, and Osborne Dustin. Development and Validation of a Complete GATE Model of the Siemens Inveon Trimodal Imaging Platform. Molecular Imaging, 12(7):7290.2013.00058, October 2013. ISSN 1536-0121. doi: 10.2310/7290.2013.00058.

[94]. Lee Sanghyeb, Gregor Jens, Kennel Stephen J., Osborne Dustin R., and Wall Jonathan. GATE Validation of Standard Dual Energy Corrections in Small Animal SPECT-CT. PLOS ONE, 10(4):e0122780, April 2015. ISSN 1932-6203. doi: 10/ghcmwb. [PubMed: 25849544]

[95]. Lee Young Sub, Kim Jin Su, Kim Kyeong Min, Lim Sang Moo, and Kim Hee-Joung. Determination of energy windows for the triple energy window scatter correction method in I-131 on a Siemens SYMBIA gamma camera: A GATE simulation study. Journal of Instrumentation, 10(01):P01004–P01004, January 2015. ISSN 1748-0221. doi: 10.1088/1748-0221/10/01/P01004.

[96]. Lehner CE, He Zhong, and Zhang Feng. 4/spl pi/ Compton imaging using a 3-D position-sensitive CdZnTe detector via weighted list-mode maximum likelihood. IEEE Transactions on Nuclear Science, 51(4):1618–1624, August 2004. ISSN 1558-1578. doi: 10/fk8gcq.

[97]. Lenz Mirjam. Design and Characterisation of an MRI Compatible Human Brain PET Insert by Means of Simulation and Experimental Studies. PhD thesis, Bergische Universität Wuppertal, 2020.

[98]. Lewellen Tom K.. Recent developments in PET detector technology. Physics in Medicine and Biology, 53(17):R287–317, September 2008. ISSN 0031-9155. doi: 10/dqvc56. [PubMed: 18695301]

[99]. Li Suying, Zhang Qiushi, Vuletic Ivan, Xie Zhaoheng, Yang Kun, and Ren Qiushi. Monte Carlo simulation of Ray-Scan 64 PET system and performance evaluation using GATE toolkit. Journal of Instrumentation, 12(02):T02001–T02001, February 2017. ISSN 1748-0221. doi: 10/ghcmwc.

[100]. Liu Zhiqiang, Fan Jiawei, Li Minghui, Yan Hui, Hu Zhihui, Huang Peng, Tian Yuan, Miao Junjie, and Dai Jianrong. A deep learning method for prediction of three-dimensional dose distribution of helical tomotherapy. Medical Physics, 46(5):1972–1983, 2019. ISSN 2473-4209. doi: 10/ggw5v3. [PubMed: 30870586]

[101]. Loudos George K., Papadimitroulas Panagiotis, Zotos Panteleimon, Tsougos Ioannis, and Georgoulias Panagiotis. Development and evaluation of QSPECT open-source software for the iterative reconstruction of SPECT images. Nuclear Medicine Communications, 31(6):558–566, June 2010. ISSN 1473-5628. doi: 10/cqz75q. [PubMed: 20351598]

[102]. Loudos George K., Papadimitroulas Panagiotis G., and Kagadis George C.. Exploitation of realistic computational anthropomorphic phantoms for the optimization of nuclear imaging acquisition and processing protocols. Conference proceedings: … Annual International Conference of the IEEE Engineering in Medicine and Biology Society. IEEE Engineering in

Medicine and Biology Society. Annual Conference, 2014:1921–1924, 2014. ISSN 1557-170X. doi: 10/ghbjxc.

[103]. Lu Lijun, Zhang Houjin, Bian Zhaoying, Ma Jianhua, Feng Qiangjin, and Chen Wufan. Validation of a Monte Carlo simulation of the Inveon PET scanner using GATE. Nuclear Instruments and Methods in Physics Research Section A: Accelerators, Spectrometers, Detectors and Associated Equipment, 828:170–175, August 2016. ISSN 0168-9002. doi: 10/ggkktt.

[104]. Asensi Madrigal Jorge Ricardo. Deep Learning Approach for Denoising Monte Carlo Dose Distribution in Proton Therapy. PhD thesis, Université Catholique de Louvain, 2018.

[105]. Maier Daniel, Blondel Claire, Delisle Cyrille, Limousin Olivier, Martignac Jérôme, Meuris Aline, Visticot François, Daniel Geoffrey, Bausson Pierre-Anne, Gevin Olivier, Amoyal Guillaume, Carrel Frédérick, Schoepff Vincent, Mahé Charly, Soufflet Fabrice, and Vassal Marie-Cécile. Second generation of portable gamma camera based on Caliste CdTe hybrid technology. Nuclear Instruments and Methods in Physics Research Section A: Accelerators, Spectrometers, Detectors and Associated Equipment, 912:338–342, December 2018. ISSN 0168-9002. doi: 10/ghhdgt.

[106]. Maxim Voichiţa. Enhancement of Compton camera images reconstructed by inversion of a conical Radon transform. Inverse Problems, 35(1):014001, 2019. doi: 10.1088/1361-6420/aaecdb.

[107]. Maybody Majid, Grewal Ravinder K, Healey John H, Antonescu Cristina R, Fanchon Louise, Hwang Sinchun, Carrasquillo Jorge A, Kirov Assen, Farooki Azeez. Ga-68 DOTATOC PET/CT Guided Biopsy and Cryoablation with Autoradiography of Biopsy Specimen for Treatment of Tumor-Induced Osteomalacia. Cardiovascular and interventional radiology, 39(9):1352–1357, September 2016. ISSN 0174-1551. doi: 10/f8w62v. [PubMed: 27150801]

[108]. McIntosh Bryan, Stout David B., and Goertzen Andrew L.. Validation of a GATE Model of $\hat{}${176}$Lu Intrinsic Radioactivity in LSO PET Systems. IEEE Transactions on Nuclear Science, 58(3):682–686, June 2011. ISSN 0018-9499, 1558-1578. doi: 10/fknr35.

[109]. Mehadji Dupont, and Morel Christian. Monte Carlo simulation of aSiPMs with GATE. J. Instrum, pages Submitted, in review, 2020.

[110]. Merheb Charbel, Nicol Stan, Petegnief Yolande, Talbot Jean-Noël, and Buvat Irène. Assessment of the Mosaic animal PET system response using list-mode data for validation of GATE Monte Carlo modelling. Nuclear Instruments and Methods in Physics Research Section A: Accelerators, Spectrometers, Detectors and Associated Equipment, 569(2):220–224, December 2006. ISSN 0168-9002. doi: 10/b7qm6h.

[111]. Merlin Thibaut, Stute Simon, Benoit Didier, Bert Julien, Carlier Thomas, Comtat Claude, Filipovic Marina, Lamare Frédéric, and Visvikis Dimitris. CASToR: A generic data organization and processing code framework for multi-modal and multi-dimensional tomographic reconstruction. Physics in Medicine and Biology, 63(18):185005, September 2018. ISSN 1361-6560. doi: 10/gg2nwz. [PubMed: 30113313]

[112]. Michel C, Eriksson L, Rothfuss H, Bendriem B, Lazaro D, and Buvat I. Influence of crystal material on the performance of the HiRez 3D PET scanner: A Monte-Carlo study. In IEEE Nuclear Science Symposium Conference Record, volume 4, pages 2528–2531, October 2006. doi: 10/cvq5vh.

[113]. Mihailescu L, Vetter KM, Burks MT, Hull EL, and Craig WW. SPEIR: A Ge Compton camera. Nuclear Instruments and Methods in Physics Research Section A: Accelerators, Spectrometers, Detectors and Associated Equipment, 570(1):89–100, January 2007. ISSN 0168-9002. doi: 10/ftp4xh.

[114]. Mok Greta S. P., Du Yong, Wang Yuchuan, Frey Eric C., and Tsui Benjamin M. W.. Development and Validation of a Monte Carlo Simulation Tool for Multi-Pinhole SPECT. Molecular Imaging and Biology, 12(3):295–304, June 2010. ISSN 1860-2002. doi: 10/dth7w5. [PubMed: 19779896]

[115]. Monnier Florian, Fayad Hadi, Bert Julien, Schmidt Holger, and Visvikis Dimitris. Validation of a simultaneous PET/MR system model for PET simulation using GATE. EJNMMI Physics, 2(1):A45, May 2015. ISSN 2197-7364. doi: 10/ghcms3. [PubMed: 26956303]

[116]. Montémont G, Bohuslav P, Dubosq J, Feret B, Monnet O, Oehling O, Skala L, Stanchina S, Verger L, and Werthmann G. NuVISION: A Portable Multimode Gamma Camera based on HiSPECT Imaging Module. In 2017 IEEE Nuclear Science Symposium and Medical Imaging Conference (NSS/MIC), pages 1–3, October 2017. doi: 10/ghhdgs.

[117]. Moraes Eder R., Poon Jonathan K., Balakrishnan Karthikayan, Wang Wenli, and Badawi Ramsey D.. Towards component-based validation of GATE: Aspects of the coincidence processor. Physica Medica, 31(1):43–48, February 2015. ISSN 1120-1797. doi: 10/f6vp94. [PubMed: 25240897]

[118]. Moskal P, Krawczyk N, Hiesmayr BC, Bała M, Curceanu C, Czerwiński E, Dulski K, Gajos A, Gorgol M, Del Grande R, Jasińska B, Kacprzak K, Kapłon L, Kisielewska D, Klimaszewski K, Korcyl G, Kowalski P, Kozik T, Krzemień W, Kubicz E, Mohammed M, Niedźwiecki Sz., Pałka M, Pawlik-Niedźwiecka M, Raczyński L, Raj J, Rudy Z, Sharma S, Silarski M, Shivani, Shopa RY, Skurzok M, Wiślicki W, Zgardzińska B. Feasibility studies of the polarization of photons beyond the optical wavelength regime with the J-PET detector. The European Physical Journal C, 78(11):970, November 2018. ISSN 1434-6052. doi: 10/ghdrdw. [PubMed: 30636927]

[119]. Moskal P, Kisielewska D, Curceanu C, Czerwiński E, Dulski K, Gajos A, Gorgol M, Hiesmayr B, Jasińska B, Kacprzak K, Kaplon L, Korcyl G, Kowalski P, Krzemień W, Kozik T, Kubicz E, Mohammed M, Niedźwiecki Sz, Palka M, Pawlik-Niedźwiecka M, Raczyński L, Raj J, Sharma S, Shivani, Shopa RY, Silarski M, Skurzok M, Stepień E, Wiślicki W, and Zgardzińska B. Feasibility study of the positronium imaging with the J-PET tomograph. Physics in Medicine & Biology, 64(5):055017, March 2019. ISSN 0031-9155. doi: 10/ghbjzz. [PubMed: 30641509]

[120]. Moskal Paweł and Stepień Ewa Ł. Prospects and Clinical Perspectives of Total-Body PET Imaging Using Plastic Scintillators. PET clinics, 15(4):439–452, October 2020. ISSN 1879-9809. doi: 10/ghdrd4. [PubMed: 32739047]

[121]. Moskal Paweł, Jasińska Bożena, Stepień Ewa Ł, and Bass Steven D. Positronium in medicine and biology. Nature Reviews Physics, 1(9):527–529, September 2019. ISSN 2522-5820. doi: 10/ghdrd8.

[122]. Mountris K, Autret A, Papadimitroulas P, Loudos G, Visvikis D, and Nikiforidis G. Optimization of Image-based Dosimetry in Y90 Radioembolization: A Monte Carlo approach using the GATE simulation toolkit. Physica Medica: European Journal of Medical Physics, 30:e47, January 2014. ISSN 1120-1797. doi: 10/ghn45s.

[123]. Müller Florian, Schug David, Hallen Patrick, Grahe Jan, and Schulz Volkmar. Gradient Tree Boosting-Based Positioning Method for Monolithic Scintillator Crystals in Positron Emission Tomography. IEEE Transactions on Radiation and Plasma Medical Sciences, 2(5):411–421, September 2018. ISSN 2469-7303. doi: 10/ghc83z.

[124]. Müller Florian, Schug David, Hallen Patrick, Grahe Jan, and Schulz Volkmar. A novel DOI Positioning Algorithm for Monolithic Scintillator Crystals in PET based on Gradient Tree Boosting. IEEE Transactions on Radiation and Plasma Medical Sciences, 3(4):465–474, July 2019. ISSN 2469-7311, 2469-7303. doi: 10/ghc8kg.

[125]. Muñoz Enrique, Barrio John, Etxebeste Ane, Ortega Pablo G, Lacasta Carlos, Oliver Josep F, Solaz Carles, and Llosá Gabriela. Performance evaluation of MACACO: A multilayer Compton camera. Physics in Medicine & Biology, 62(18):7321–7341, August 2017. ISSN 1361-6560. doi: 10/gf685p. [PubMed: 28718772]

[126]. Muñoz Enrique, Barrio John, Bernabéu José, Etxebeste Ane, Lacasta Carlos, Llosá Gabriela, Ros Ana, Roser Jorge, and Oliver Josep F.. Study and comparison of different sensitivity models for a two-plane Compton camera. Physics in Medicine & Biology, 63(13):135004, June 2018. ISSN 0031-9155. doi: 10/ghj5vt. [PubMed: 29847316]

[127]. Neph Ryan, Huang Yangsibo, Yang Youming, and Sheng Ke. DeepMCDose: A Deep Learning Method for Efficient Monte Carlo Beamlet Dose Calculation by Predictive Denoising in MR-Guided Radiotherapy. In Nguyen Dan, Xing Lei, and Jiang Steve, editors, Artificial Intelligence in Radiation Therapy, volume 11850, pages 137–145. Springer International Publishing, Cham, 2019. ISBN 978-3-030-32485-8 978-3-030-32486-5. doi: 10.1007/978-3-030-32486-5_17.

[128]. Nguyen Dan, Jia Xun, Sher David, Lin Mu-Han, Iqbal Zohaib, Liu Hui, and Jiang Steve. 3D radiotherapy dose prediction on head and neck cancer patients with a hierarchically densely

connected U-net deep learning architecture. Physics in Medicine and Biology, 64(6):065020, March 2019. ISSN 1361-6560. doi: 10/ggw5v2. [PubMed: 30703760]

[129]. Nikolopoulos Dimitrios, Kottou Sofia, Chatzisavvas Nikolaos, Argyriou Xenophon, Vlamakis Emannouel, Yannakopoulos Panayiotis, and Louizi Anna. A GATE Simulation Study of the Siemens Biograph DUO PET/CT System. Open Journal of Radiology, 2013:56–65, June 2013. doi: 10/ghck68.

[130]. Oliver Josep F., Fuster-Garcia Elies, Cabello Jorge, Tortajada Salvador, and Rafecas Magdalena. Application of Artificial Neural Network for Reducing Random Coincidences in PET. IEEE Transactions on Nuclear Science, 60(5):3399–3409, October 2013. ISSN 1558-1578. doi: 10/f5c7p5.

[131]. Papadimitroulas Panagiotis, Loudos George, Nikiforidis George C., and Kagadis George C.. A dose point kernel database using GATE Monte Carlo simulation toolkit for nuclear medicine applications: Comparison with other Monte Carlo codes. Med Phys, 39(8):5238–5247, August 2012. doi: 10.1118/1.4737096. [PubMed: 22894448]

[132]. Park Min-Jae, Park Kwang-Suk, Lee Jae-Sung, Kim Yu-Kyeong, and Lee Dong-Soo. Validation of a GATE Model for the Simulation of a Trionix TRIAD SPECT Camera. JOURNAL OF THE KOREAN PHYSICAL SOCIETY, 2009. ISSN 0374-4884. doi: 10/ffvdxt.

[133]. Paszke Adam, Gross Sam, Massa Francisco, Lerer Adam, Bradbury James, Chanan Gregory, Killeen Trevor, Lin Zeming, Gimelshein Natalia, Antiga Luca, Desmaison Alban, Kopf Andreas, Yang Edward, DeVito Zachary, Raison Martin, Tejani Alykhan, Chilamkurthy Sasank, Steiner Benoit, Fang Lu, Bai Junjie, and Chintala Soumith. PyTorch: An Imperative Style, High-Performance Deep Learning Library. NEURIPS 2019, page 12, 2019.

[134]. Pedemonte Stefano, Pierce Larry, and Van Leemput Koen. A machine learning method for fast and accurate characterization of depth-of-interaction gamma cameras. Physics in Medicine & Biology, 62(21):8376–8401, October 2017. ISSN 1361-6560. doi: 10/ghc9pv. [PubMed: 28436919]

[135]. Peng Zhao, Shan Hongming, Liu Tianyu, Pei Xi, Zhou Jieping, Wang Ge, and Xu X. George. Deep learning for accelerating Monte Carlo radiation transport simulation in intensity-modulated radiation therapy. arXiv:1910.07735 [physics], October 2019.

[136]. Pivarski Jim, Das Pratyush, Burr Chris, Smirnov Dmitri, Feickert Matthew, Gal Tamas, Kreczko Luke, Smith Nicholas, Biederbeck Noah, Shadura Oksana, Proffitt Mason, benkrikler, Dembinski Hans, Schreiner Henry, Rembser Jonas, R. Marcel, Gu Chao, Rübenach Jonas, Peresano Michele, and Turra Ruggero. Scikit-hep/uproot: 3.12.0. Zenodo, July 2020.

[137]. Poon Jonathan K., Dahlbom Magnus L., Moses William W., Balakrishnan Karthik, Wang Wenli, Cherry Simon R., and Badawi Ramsey D.. Optimal whole-body PET scanner configurations for different volumes of LSO scintillator: A simulation study. Physics in Medicine and Biology, 57(13):4077–4094, July 2012. ISSN 1361-6560. doi: 10/ggkktv. [PubMed: 22678106]

[138]. Poon Jonathan K., Dahlbom Magnus L., Casey Michael E., Qi Jinyi, Cherry Simon R., and Badawi Ramsey D.. Validation of the SimSET simulation package for modeling the Siemens Biograph mCT PET scanner. Physics in Medicine and Biology, 60(3):N35–N45, January 2015. ISSN 0031-9155. doi: 10/ghcrjf. [PubMed: 25586800]

[139]. Ramos E, Kochebina O, Yvon D, Verrecchia P, Sharyy V, Tauzin G, Mols JP, Starzinski P, Desforges D, Flouzat Ch, Bulbul Y, Jan S, Mancardi X, Canot C, and Alokhina M. Efficient and fast 511-keV $\upgamma$ detection through Cherenkov radiation: The CaLIPSO optical detector. Journal of Instrumentation, 11(11):P11008–P11008, November 2016. ISSN 1748-0221. doi: 10/gh58pw.

[140]. Rannou Fernando R., Kohli Vandana, Prout David L., and Chatziioannou Arion F.. Investigation of OPET Performance Using GATE, a Geant4-Based Simulation Software. IEEE transactions on nuclear science, 51(5):2713–2717, October 2004. ISSN 0018-9499. doi: 10/dr6fbp. [PubMed: 16429604]

[141]. Reader AJ, Corda G, Mehranian A, da Costa-Luis C, Ellis S, and Schnabel JA. Deep Learning for PET Image Reconstruction. IEEE Transactions on Radiation and Plasma Medical Sciences, pages 1–1, 2020. ISSN 2469-7303. doi: 10/ghbzfs.

[142]. Rechka Sanae, Fontaine RÁjean, Rafecas Magdalena, and Lecomte Roger. Development and Validation of a GATE Simulation Model for the LabPET Scanner. IEEE Transactions on Nuclear Science, 56(6):3672–3679, December 2009. ISSN 1558-1578. doi: 10/dhchrk.

[143]. Rehfeld Niklas S., Stute Simon, Apostolakis John, Soret Marine, and Buvat Irène. Introducing improved voxel navigation and fictitious interaction tracking in GATE for enhanced efficiency. Physics in Medicine and Biology, 54(7):2163–2178, March 2009. ISSN 0031-9155. doi: 10/fkg9jc. [PubMed: 19293466]

[144]. Rey M, Jan S, Vieira JM, Mosset JB, Krieguer M, Comtat C, and Morel C. Count rate performance study of the Lausanne ClearPET scanner demonstrator. Nuclear Instruments and Methods in Physics Research Section A: Accelerators, Spectrometers, Detectors and Associated Equipment, 571(1):207–210, February 2007. ISSN 0168-9002. doi: 10/bqxjcv.

[145]. Ricci Rita, Kostou Theodora, Chatzipapas Konstantinos, Fysikopoulos Eleftherios, Loudos George, Montalto Luigi, Scalise Lorenzo, Rinaldi Daniele, and David Stratos. Monte Carlo Optical Simulations of a Small FoV Gamma Camera. Effect of Scintillator Thicknesses and Septa Materials. Crystals, 9(8):398, August 2019. doi: 10/ghcjfv.

[146]. Rit S, Vila Oliva M, Brousmiche S, Labarbe R, Sarrut D, and Sharp GC. The Reconstruction Toolkit (RTK), an open-source cone-beam CT reconstruction toolkit based on the Insight Toolkit (ITK). Journal of Physics: Conference Series, 489:012079, March 2014. ISSN 1742-6596. doi: 10/ggjtjg.

[147]. Robert Antoine, Rit Simon, Baudier Thomas, Jomier Julien, and Sarrut David. 4D respiration-correlated whole-body SPECT reconstruction. In 2019 IEEE NSS-MIC, 2019.

[148]. Robert Antoine, Rit Simon, Baudier Thomas, Jomier Julien, and Sarrut David. 4D respiration-correlated whole-body SPECT reconstruction. Phys Med Biol, pages Submitted, in review, 2020.

[149]. Robert Charlotte, Montémont Guillaume, Rebuffel Véronique, Verger Loïck, and Buvat Irène. Optimization of a parallel hole collimator/CdZnTe gamma-camera architecture for scintimammography. Medical Physics, 38(4):1806–1819, 2011. ISSN 2473-4209. doi: 10/bdvfzp. [PubMed: 21626915]

[150]. Roncali Emilie and Cherry Simon R.. Application of silicon photomultipliers to positron emission tomography. Annals of Biomedical Engineering, 39(4):1358–1377, April 2011. ISSN 1573-9686. doi: 10/fs2hbd. [PubMed: 21321792]

[151]. Roncali Emilie and Cherry Simon R.. Simulation of light transport in scintillators based on 3D characterization of crystal surfaces. Physics in Medicine and Biology, 58(7):2185–2198, April 2013. ISSN 1361-6560. doi: 10/gh3sgq. [PubMed: 23475145]

[152]. Roncali Emilie, Kwon Sun Il, Jan Sebastien, Berg Eric, and Cherry Simon R.. Cerenkov light transport in scintillation crystals explained: Realistic simulation with GATE. Biomedical Physics & Engineering Express, 5(3):035033, April 2019. ISSN 2057-1976. doi: 10/ghbjz3. [PubMed: 33304614]

[153]. Roncali Emilie, Taebi Amirtahà, Foster Cameron, and Vu Catherine Tram. Personalized Dosimetry for Liver Cancer Y-90 Radioembolization Using Computational Fluid Dynamics and Monte Carlo Simulation. Annals of Biomedical Engineering, 48(5):1499–1510, May 2020. ISSN 1573-9686. doi: 10/ghn45r. [PubMed: 32006268]

[154]. Roshan Hoda Rezaei, Mahmoudian Babak, Gharepapagh Esmaeil, Azarm Ahmadreza, and Islamian Jalil Pirayesh. Collimator and energy window optimization for ^{90}Y bremsstrahlung SPECT imaging: A SIMIND Monte Carlo study. Applied Radiation and Isotopes: Including Data, Instrumentation and Methods for Use in Agriculture, Industry and Medicine, 108:124–128, February 2016. ISSN 1872-9800. doi: 10/f785sx. [PubMed: 26720261]

[155]. Sadremomtaz Alireza and Telikani Zeinab. Validation and optimization studies of small animal SPECT using GATE Monte Carlo simulation. Nuclear Instruments and Methods in Physics Research Section A: Accelerators, Spectrometers, Detectors and Associated Equipment, 915:94–101, January 2019. ISSN 0168-9002. doi: 10/ghcmwd.

[156]. Sajedi Salar, Blackberg Lisa, El Fakhri Georges, Choi Hak Soo, and Sabet Hamid. Intraoperative radio-guided imaging system for surgical applications. Journal of Nuclear Medicine, 60(supplement 1):317–317, May 2019. ISSN 0161-5505, 2159-662X.

[157]. Sakellios Nikolas, Rubio Jose Luis, Karakatsanis Nicolas, Kontaxakis George, Loudos George, Santos Andres, Nikita Konstantina, and Majewski Stan. GATE simulations for small animal

SPECT/PET using voxelized phantoms and rotating-head detectors. In 2006 IEEE Nuclear Science Symposium Conference Record, volume 4, pages 2000–2003, October 2006. doi: 10/fwtjz9.

[158]. Salvadori Julien, Labour Joey, Odille Freddy, Marie Pierre-Yves, Badel Jean-Noël, Imbert Laëtitia, and Sarrut David. Monte Carlo simulation of digital photon counting PET. EJNMMI physics, 7(1):23, April 2020. ISSN 2197-7364. doi: 10/ggw5vb. [PubMed: 32335787]

[159]. Santin G, Strul D, Lazaro D, Simon L, Krieguer M, Martins MV, Breton V, and Morel C. GATE: A Geant4-based simulation platform for PET and SPECT integrating movement and time management. IEEE Transactions on Nuclear Science, 50(5):1516–1521, October 2003. ISSN 1558-1578. doi: 10/cx6xp2.

[160]. Sarrut D, Krah N, Badel JN, and Létang JM. Learning SPECT detector angular response function with neural network for accelerating Monte-Carlo simulations. Physics in Medicine & Biology, 63(20):205013, October 2018. ISSN 1361-6560. doi: 10/ggjtkb. [PubMed: 30238925]

[161]. Sarrut D, Krah N, and Létang JM. Generative adversarial networks (GAN) for compact beam source modelling in Monte Carlo simulations. Physics in Medicine & Biology, 64(21):215004, October 2019. ISSN 0031-9155. doi: 10/gf82xv. [PubMed: 31470418]

[162]. Sarrut David, Bardiès Manuel, Boussion Nicolas, Freud Nicolas, Jan Sébastien, Létang Jean-Michel, Loudos George, Maigne Lydia, Marcatili Sara, Mauxion Thibault, et al. A review of the use and potential of the GATE Monte Carlo simulation code for radiation therapy and dosimetry applications. Medical physics, 41(6Part1):064301, June 2014. doi: 10.1118/1.4871617. [PubMed: 24877844]

[163]. Schaart Dennis R., Ziegler Sibylle, and Zaidi Habib. Achieving 10 ps coincidence time resolution in TOF-PET is an impossible dream. Medical Physics, 47(7):2721–2724, 2020. ISSN 2473-4209. doi: 10/ghfrj6. [PubMed: 32141611]

[164]. Scheins JJ and Herzog H. PET Reconstruction Software Toolkit - PRESTO a novel, universal C++ library for fast, iterative, fully 3D PET image reconstruction using highly compressed, memory-resident system matrices. In 2008 IEEE Nuclear Science Symposium Conference Record, pages 4147–4150, October 2008. doi: 10/bqjdpk.

[165]. Scheins JJ, Herzog H, and Shah NJ. Fully-3D PET image reconstruction using scanner-independent, adaptive projection data and highly rotation-symmetric voxel assemblies. IEEE transactions on medical imaging, 30(3):879–892, March 2011. ISSN 1558-254X. doi: 10/bzk2cn. [PubMed: 21292592]

[166]. Scheins JJ, Vahedipour K, Pietrzyk U, and Shah NJ. High performance volume-of-intersection projectors for 3D-PET image reconstruction based on polar symmetries and SIMD vectorisation. Physics in Medicine and Biology, 60(24):9349–9375, December 2015. ISSN 1361-6560. doi: 10/gh3sgs. [PubMed: 26579597]

[167]. Schmidtlein C. Ross, Kirov Assen S., Nehmeh Sadek A., Erdi Yusuf E., Humm John L., Amols Howard I., Bidaut Luc M., Ganin Alex, Stearns Charles W., McDaniel David L., and Hamacher Klaus A.. Validation of GATE Monte Carlo simulations of the GE Advance/Discovery LS PET scanners. Medical Physics, 33(1):198–208, January 2006. ISSN 0094-2405. doi: 10/cgngq8. [PubMed: 16485426]

[168]. Schüffler Peter J., Fuchs Thomas J., Ong Cheng Soon, Wild Peter J., Rupp Niels J., and Buhmann Joachim M.. TMARKER: A free software toolkit for histopathological cell counting and staining estimation. Journal of Pathology Informatics, 4(Suppl):S2, 2013. ISSN 2229-5089. doi: 10/ghn45q. [PubMed: 23766938]

[169]. Seiter Daniel, Schüffler Peter J., Dogan Snjezana, Popovic Marko, Turkekul Mesruh, Christian Czmielewski, Schmidtlein Charles, Manova-Todorova Katia, Humm John, Fuchs Thomas, Solomon Stephen, and Kirov Assen. Quantity and location of the tumor cells in a biopsy specimen. Journal of Nuclear Medicine, 59(supplement 1):248–248, May 2018. ISSN 0161-5505, 2159-662X.

[170]. Sheikhzadeh Peyman, Sabet Hamid, Ghadiri Hossein, Geramifar Parham, Mahani Hojjat, Ghafarian Pardis, and Ay Mohammad Reza. Development and validation of an accurate GATE model for NeuroPET scanner. Physica Medica, 40:59–65, August 2017. ISSN 1120-1797. doi: 10/gbzmmp. [PubMed: 28716541]

[171]. Shibuya Kengo, Saito Haruo, Nishikido Fumihiko, Takahashi Miwako, and Yamaya Taiga. Oxygen sensing ability of positronium atom for tumor hypoxia imaging. Communications Physics, 3(1):1–8, October 2020. ISSN 2399-3650. doi: 10/ghf3zq.

[172]. Solevi P, Oliver JF, Gillam JE, Bolle E, Casella C, Chesi E, De Leo R, Dissertori G, Fanti V, Heller M, Lai M, Lustermann W, Nappi E, Pauss F, Rudge A, Ruotsalainen U, Schinzel D, Schneider T, Séguinot J, Stapnes S, Weilhammer P, Tuna U, Joram C, and Rafecas M. A Monte-Carlo based model of the AX-PET demonstrator and its experimental validation. Physics in Medicine and Biology, 58(16):5495–5510, July 2013. ISSN 0031-9155. doi: 10/ghcmwf. [PubMed: 23880523]

[173]. Somlai-Schweiger I and Ziegler SI. CHERENCUBE: Concept definition and implementation challenges of a Cherenkov-based detector block for PET. Medical Physics, 42(4):1825–1835, April 2015. ISSN 2473-4209. doi: 10/f68cks. [PubMed: 25832073]

[174]. Song X, Segars WP, Du Y, Tsui BMW, and Frey EC. Fast modelling of the collimator–detector response in Monte Carlo simulation of SPECT imaging using the angular response function. Physics in Medicine and Biology, 50(8):1791–1804, April 2005. ISSN 0031-9155, 1361-6560. doi: 10/d6rjs6. [PubMed: 15815096]

[175]. Spadola S, Verdier M-A, Pinot L, Esnault C, Dinu N, Charon Y, Duval M-A, and Ménard L. Design optimization and performances of an intraoperative positron imaging probe for radioguided cancer surgery. Journal of Instrumentation, 11(12):P12019, December 2016. ISSN 1748-0221. doi: 10/ghn45v.

[176]. Spirou Spiridon V., Papadimitroulas Panagiotis, Liakou Paraskevi, Georgoulias Panagiotis, and Loudos George. Investigation of attenuation correction in SPECT using textural features, Monte Carlo simulations, and computational anthropomorphic models. Nuclear Medicine Communications, 36(9):952–961, September 2015. ISSN 1473-5628. doi: 10/ghbjxf. [PubMed: 26011587]

[177]. Staelens S, Koole M, Vandenberghe S, D'Asseler Y, Lemahieu I, and Van de Walle R. The geometric transfer function for a slat collimator mounted on a strip detector. IEEE Transactions on Nuclear Science, 52(3):708–713, June 2005. ISSN 1558-1578. doi: 10/dr25rs.

[178]. Staelens Steven, Strul Daniel, Santin Giovanni, Vandenberghe Stefaan, Koole Michel, D'Asseler Yves, Lemahieu Ignace, and Van de Walle Rik. Monte Carlo simulations of a scintillation camera using GATE: Validation and application modelling. Physics in medicine and biology, 48(18):3021–3042, September 2003. ISSN 0031-9155. [PubMed: 14529208]

[179]. Staelens Steven, Vunckx Kathleen, De Beenhouwer Jan, Beekman Freek, D'Asseler Yves, Nuyts Johan, and Lemahieu Ignace. GATE simulations for optimization of pinhole imaging. Nuclear Instruments and Methods in Physics Research Section A: Accelerators, Spectrometers, Detectors and Associated Equipment, 569(2):359–363, December 2006. ISSN 0168-9002. doi: 10/bc2hhf.

[180]. Stockhoff Mariele, Jan Sebastien, Dubois Albertine, Cherry Simon R., and Roncali Emilie. Advanced optical simulation of scintillation detectors in GATE V8.0: First implementation of a reflectance model based on measured data. Physics in Medicine and Biology, 62(12):L1–L8, June 2017. ISSN 1361-6560. doi: 10/ghbjz5. [PubMed: 28452339]

[181]. Stockhoff Mariele, Van Holen Roel, and Vandenberghe Stefaan. Optical simulation study on the spatial resolution of a thick monolithic PET detector. Physics in Medicine and Biology, 64(19):195003, September 2019. ISSN 1361-6560. doi: 10/ghbjz4. [PubMed: 31416055]

[182]. Strul Daniel, Santin Giovanni, Lazaro Delphine, Breton Vincent, and Morel Christian. GATE (geant4 application for tomographic emission): A PET/SPECT general-purpose simulation platform. Nuclear Physics B - Proceedings Supplements, 125:75–79, September 2003. ISSN 0920-5632. doi: 10/fhqw8c.

[183]. Strydhorst Jared and Buvat Irène. Redesign of the GATE PET coincidence sorter. Physics in Medicine and Biology, 61(18):N522–N531, September 2016. ISSN 0031-9155, 1361-6560. doi: 10/ggw5vg. [PubMed: 27589353]

[184]. Strydhorst Jared, Carlier Thomas, Dieudonné Arnaud, Conti Maurizio, and Buvat Irène. A gate evaluation of the sources of error in quantitative 90Y PET. Medical Physics, 43(10):5320, October 2016. ISSN 2473-4209. doi: 10/f9jsq8.

[185]. Surti Suleman, Del Guerra Alberto, and Zaidi Habib. Total-body PET is ready for prime time. Medical Physics, n/a(n/a), 2020. ISSN 2473-4209. doi: 10/ghgmxh.

[186]. Tabacchini V, Westerwoudt V, Borghi G, Seifert S, and Schaart DR. Probabilities of triggering and validation in a digital silicon photomultiplier. Journal of Instrumentation, 9(06):P06016–P06016, June 2014. ISSN 1748-0221. doi: 10/ghdrrm.

[187]. Taherparvar Payvand and Sadremomtaz Alireza. Development of GATE Monte Carlo simulation for a CsI pixelated gamma camera dedicated to high resolution animal SPECT. Australasian Physical & Engineering Sciences in Medicine, 41(1):31–39, March 2018. ISSN 1879-5447. doi: 10/ghcmv8. [PubMed: 29230656]

[188]. Teräs M, Tolvanen T, Johansson JJ, Williams JJ, and Knuuti J. Performance of the new generation of whole-body PET/CT scanners: Discovery STE and Discovery VCT. European Journal of Nuclear Medicine and Molecular Imaging, 34(10):1683–1692, October 2007. ISSN 1619-7089. doi: 10/dcjqzx. [PubMed: 17661031]

[189]. Thielemans Kris, Tsoumpas Charalampos, Mustafovic Sanida, Beisel Tobias, Aguiar Pablo, Dikaios Nikolaos, and Jacobson Matthew W.. STIR: Software for tomographic image reconstruction release 2. Physics in Medicine and Biology, 57(4):867–883, January 2012. ISSN 0031-9155. doi: 10/fx689h. [PubMed: 22290410]

[190]. Trigila Carlotta. Development of a Portable Gamma Imaging System for Absorbed Radiation Dose Control in Molecular Radiotherapy. PhD thesis, Université Paris-Saclay, 2019.

[191]. Trindade Andreia, Rodrigues Pedro, Perkins Amy E., Miller Michael A., Narayanan Manoj, Griesmer Jerome, Tung Chi-Hua, Zhang Bin, Shao Lingxiong, Laurence Thomas, Solf Torsten, and Wieczorek Herfried. Validation of GATE Monte Carlo simulations of the Philips GEMINI TF and TruFlight Select PET/CT scanners based on NEMA NU2 standards. In 2012 IEEE Nuclear Science Symposium and Medical Imaging Conference Record (NSS/MIC), pages 2546–2549, October 2012. doi: 10/ghcmvt.

[192]. van der Heyden Brent, Uray Martin, Fonseca Gabriel Paiva, Huber Philipp, Us Defne, Messner Ivan, Law Adam, Parii Anastasiia, Reisz Niklas, Rinaldi Ilaria, Freixas Gloria Vilches, Deutschmann Heinz, Verhaegen Frank, and Steininger Philipp. A Monte Carlo based scatter removal method for non-isocentric cone-beam CT acquisitions using a deep convolutional autoencoder. Physics in Medicine & Biology, 65(14):145002, July 2020. ISSN 0031-9155. doi: 10.1088/1361-6560/ab8954. [PubMed: 32294626]

[193]. van der Laan DJ, Maas MC, de Jong HWAM, Schaart DR, Bruyndonckx P, Lemaître C, and van Eijk CWE. Simulated performance of a small-animal PET scanner based on monolithic scintillation detectors. Nuclear Instruments and Methods in Physics Research Section A: Accelerators, Spectrometers, Detectors and Associated Equipment, 571(1):227–230, February 2007. ISSN 0168-9002. doi: 10/dn5dhp.

[194]. van Oosterom Matthias N., Meershoek Philippa, Welling Mick M., Pinto Francisco, Matthies Philipp, Simon Herve, Wendler Thomas, Navab Nassir, van de Velde Cornelis J. H., van der Poel Henk G., and van Leeuwen Fijs W. B.. Extending the Hybrid Surgical Guidance Concept With Freehand Fluorescence Tomography. IEEE transactions on medical imaging, 39(1):226–235, January 2020. ISSN 1558-254X. doi: 10/ghn45x. [PubMed: 31247546]

[195]. Vandenberghe Stefaan. Three-dimensional positron emission tomography imaging with 124I and 86Y. Nuclear Medicine Communications, 27(3):237–245, March 2006. ISSN 0143-3636. doi: 10/dn8s38. [PubMed: 16479243]

[196]. Vandenberghe Stefaan, Daube-Witherspoon Margaret E., Lewitt Robert M., and Karp Joel S.. Fast reconstruction of 3D time-of-flight PET data by axial rebinning and transverse mashing. Physics in Medicine and Biology, 51(6):1603–1621, March 2006. ISSN 0031-9155. doi: 10/bg8x7q. [PubMed: 16510966]

[197]. Vandenberghe Stefaan, Van Holen Roel, Staelens Steven, and Lemahieu Ignace. System characteristics of SPECT with a slat collimated strip detector. Physics in Medicine and Biology, 51(2):391–405, January 2006. ISSN 0031-9155. doi: 10/b8sxd3. [PubMed: 16394346]

[198]. Vandenberghe Stefaan, Mikhaylova Ekaterina, Brans Boudewijn, Defrise Michel, Lahoutte Tony, Muylle Kristoff, Van Holen Roel, Schaart Dennis, and Karp Joel. PET20.0: a cost efficient, 2mm spatial resolution Total Body PET with point sensitivity up to 22% and adaptive axial FOV

of maximum 2.00m. In Annual Congress of the European Association of Nuclear Medicine, volume Volume 44, Supplement 2, page 305, 2017. doi: 10/gcz99h.

[199]. Vandenberghe Stefaan, Moskal Pawel, and Karp Joel S.. State of the art in total body PET. EJNMMI Physics, 7(1):35, May 2020. ISSN 2197-7364. doi: 10/ghbjxj. [PubMed: 32451783]

[200]. Vandervoort Eric, Camborde Marie-Laure, Jan Sébastien, and Sossi Vesna. Monte Carlo modelling of singles-mode transmission data for small animal PET scanners. Physics in Medicine and Biology, 52(11):3169–3184, May 2007. ISSN 0031-9155. doi: 10/fjmxsc. [PubMed: 17505096]

[201]. Vetter C, Lasser T, Okur A, and Navab N. 1D-3D Registration for Intra-Operative Nuclear Imaging in Radio-Guided Surgery. IEEE Transactions on Medical Imaging, 34(2):608–617, February 2015. ISSN 1558-254X. doi: 10/ghn45z. [PubMed: 25343756]

[202]. Visvikis D, Lefevre T, Lamare F, Kontaxakis G, Santos A, and Darambara D. Monte Carlo based performance assessment of different animal PET architectures using pixellated CZT detectors. Nuclear Instruments and Methods in Physics Research Section A: Accelerators, Spectrometers, Detectors and Associated Equipment, 569(2):225–229, December 2006. ISSN 0168-9002. doi: 10/ckjvcp.

[203]. Visvikis Dimitris, Merlin Thibaut, Bousse Alexandre, Benoit Didier, and Laurent Benoit. Visvikis D, Merlin T, Bousse A, Benoit D, Laurent B, Deep learning based scatter correction for PET imaging, Eur J Nucl Med Mol Im, 47(suppl 1), S484. In *Eur J Nucl Med Mol Im*, volume 47 (suppl 1), page S484, 2020.

[204]. Xu Hancong, Lenz Mirjam, Caldeira Liliana, Ma Bo, Pietrzyk Uwe, Lerche Christoph, Shah N. Jon, and Scheins Juergen. Resolution modeling in projection space using a factorized multi-block detector response function for PET image reconstruction. Physics in Medicine & Biology, 64(14):145012, July 2019. ISSN 0031-9155. doi: 10/gh3sgr. [PubMed: 31158824]

[205]. Yang CC, Seidel J, Wang Y, Lee JS, Pomper MG, and Tsui BMW. Validation of GATE Monte Carlo simulation of the performance characteristics of a GE eXplore VISTA small animal PET system. In 2007 IEEE Nuclear Science Symposium Conference Record, volume 4, pages 3187–3190, October 2007. doi: 10/bptr6c.

[206]. Yang Ting-Yi. Machine Learning for High Resolution 3D Positioning of Gamma-Interactions in Monolithic PET Detectors. Master Thesis, Ghent University, 2019.

[207]. Yvon D, Sharyy V, Follin M, Bard J-P, Breton D, Maalmi J, Morel C, and Delagnes E. Design study of a scintronic crystal targeting tens of picoseconds time resolution for gamma ray imaging: The ClearMind detector. arXiv:2006.14855 [physics], June 2020.

[208]. Zagni F, D'Ambrosio D, Spinelli AE, Cicoria G, Fanti S, and Marengo M. Accurate modeling of a DOI capable small animal PET scanner using GATE. Applied Radiation and Isotopes, 75:105–114, May 2013. ISSN 0969-8043. doi: 10/f4vrpg. [PubMed: 23501360]

[209]. Zatcepin Artem, Pizzichemi Marco, Polesel Andrea, Paganoni Marco, Auffray Etiennette, Ziegler Sibylle I., and Omidvari Negar. Improving depth-of-interaction resolution in pixellated PET detectors using neural networks. Physics in Medicine & Biology, 65(17):175017, August 2020. ISSN 0031-9155. doi: 10/ghc3sg. [PubMed: 32570223]

[210]. Zvolský M, Schreiner N, Seeger S, Schaar M, Rakers S, and Rafecas M. Digital Zebrafish Phantom based on Micro-CT Data for Imaging Research. In 2019 IEEE Nuclear Science Symposium and Medical Imaging Conference (NSS/MIC), pages 1–2, October 2019. doi: 10/gh58pz.

[211]. Zvolský M, Seeger S, Schaar M, Schmidt C, and Rafecas M. MERMAID - A PET Prototype for Small Aquatic Animal Imaging. In 2019 IEEE Nuclear Science Symposium and Medical Imaging Conference (NSS/MIC), pages 1–2, October 2019. doi: 10/gh58px.

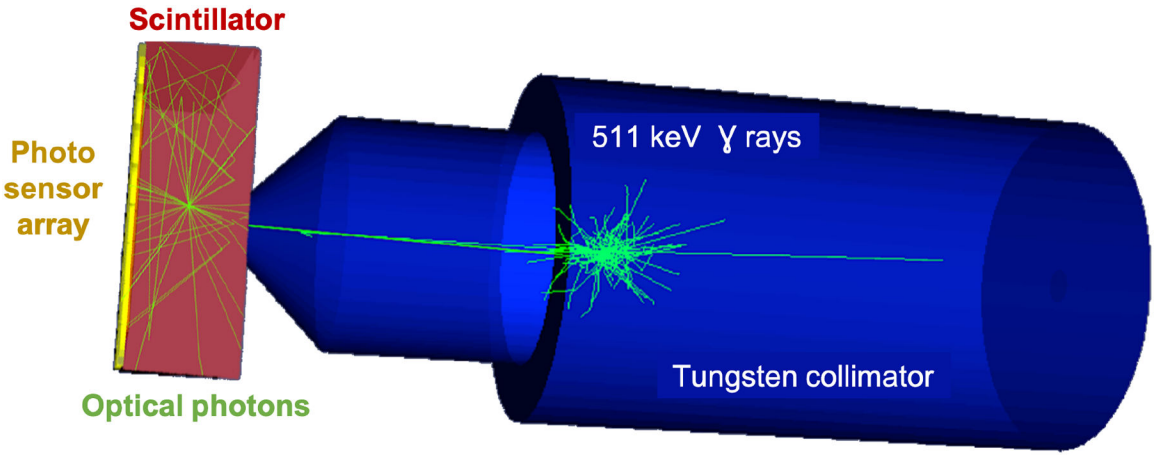

Figure 1.

Optical simulations of a calibration setup for monolithic scintillators. A 50 × 50 × 16 mm^3 LYSO crystal was modelled read out by a pixelated array of photo-detectors. The scintillator surfaces are defined by the LUT Davis reflection model based on measured data. The calibration beam is encapsulated in a tungsten collimator which is simulated by importing the 3D STL file into GATE. The source is a monoenergetic 511 keV gamma point source.

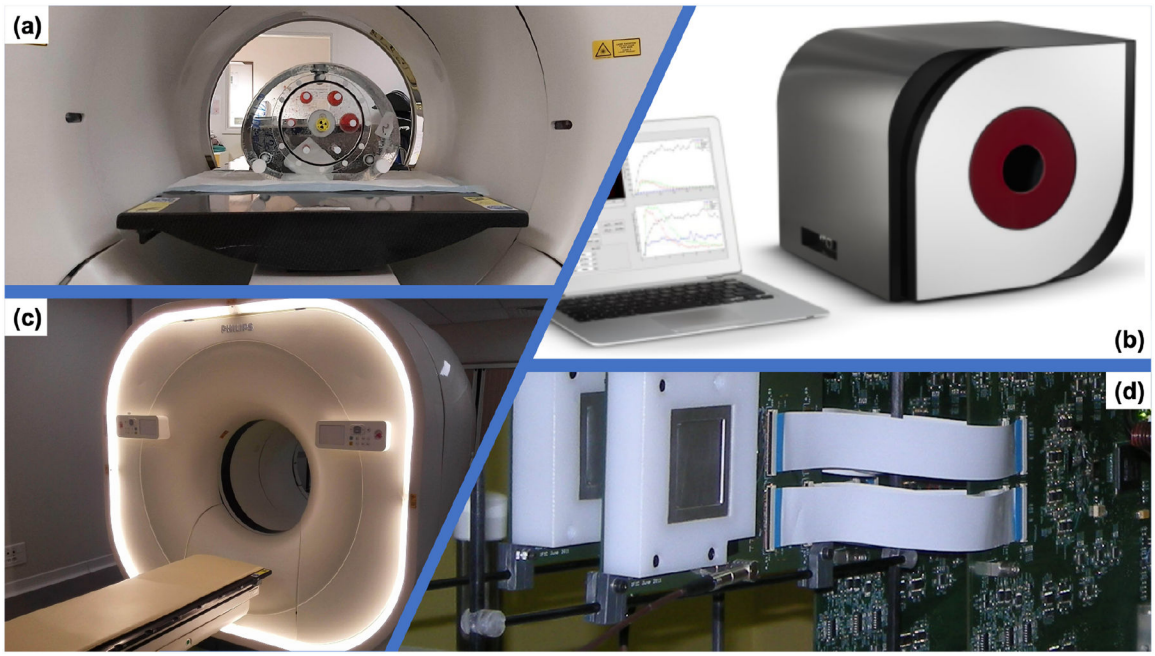

Figure 2.

Examples of some simulated imaging systems (clinical, pre-clinical, prototype). (a) NEMA IEC Body Phantom Set ready to be imaged on a PET/CT. (b) The Bioemtech γ-eye preclinical device. (c) Philips Vereos Digital PET/CT; (d) MACACO Compton Camera prototype with 2 layers of $LaBr_3$ monolithic crystals coupled to SiPMs, developed by IFIC-Valencia.

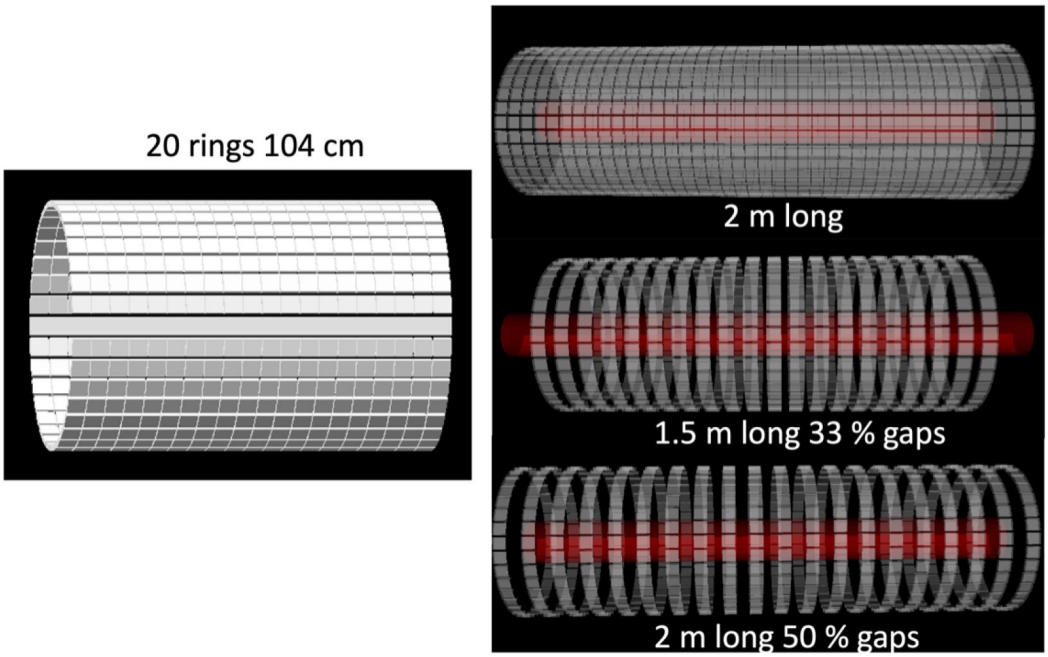

Figure 3.
(Left) A long axial FOV scanner of 20 rings (104 cm axial length) based on monolithic scintillator blocks. (right) Long axial FOV systems of 2 m with full coverage, 1.5 m with 33% gaps and a 2 m long system with 50% gaps.

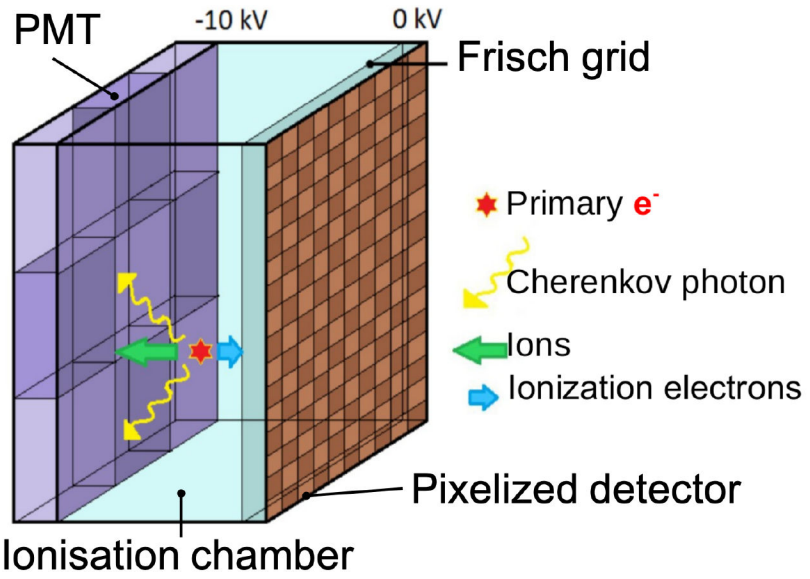

Figure 4.
Illustration of unit detector module based on the ionisation chamber filled with trimethyl bismuth (TMBi).

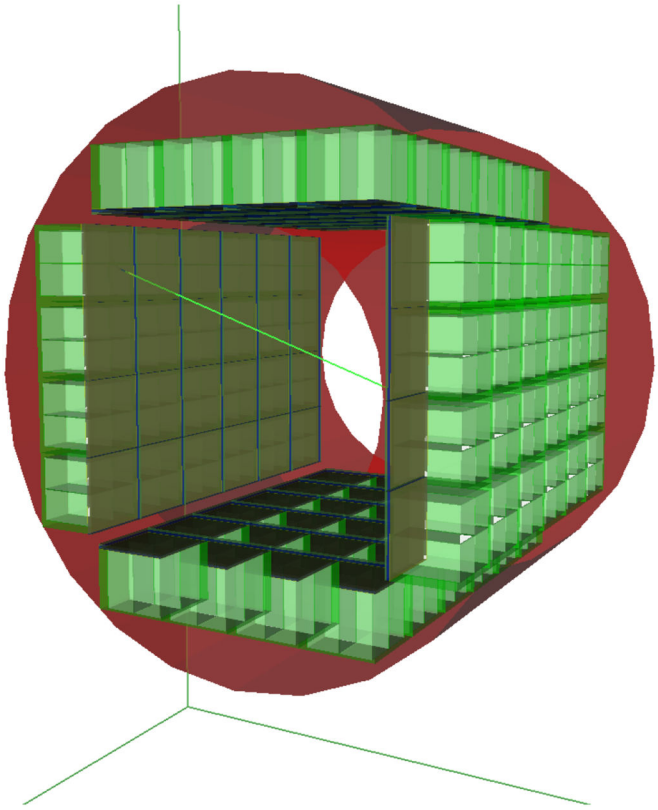

Figure 5.
Design of the CaLIPSO PET scanner dedicated for high resolution brain imaging.

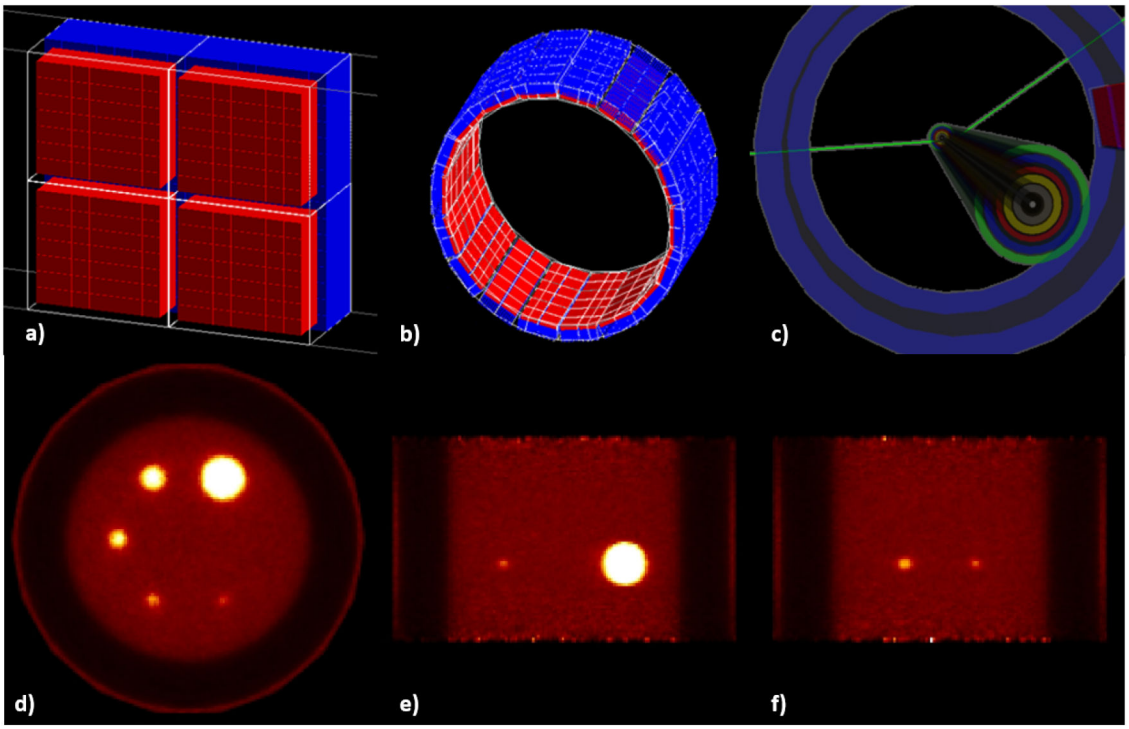

Figure 6.

Presentation of the a) modeled module of the system (1st layer in red and 2nd layer in blue), b) scheme of the full TRIMAGE scanner in GATE, c) view of the simulated phantom geometry for the sensitivity measurements (the several layers of the sleeves are presented with different colors) and d-f) transversal, coronal and sagittal slices of the 10 iterations of the simulated IQ phantom.

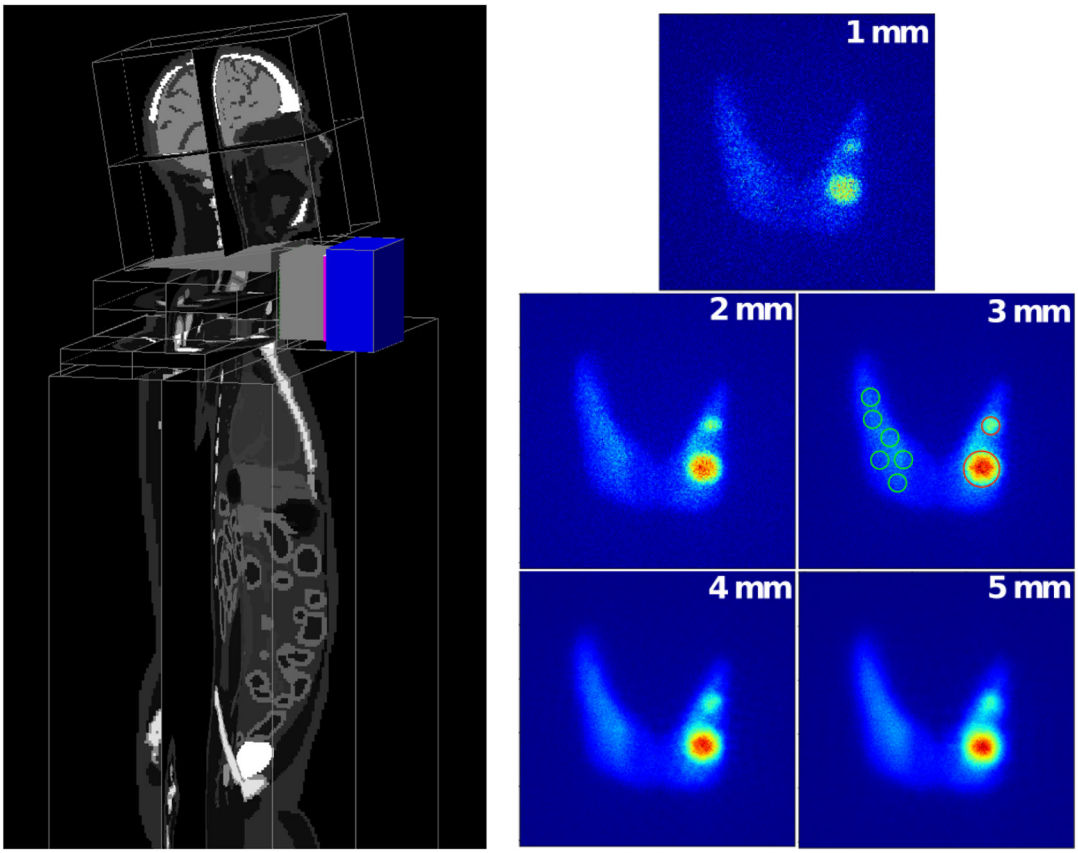

Figure 7.

Simulation set-up used for the choice of the collimator. Left - the complete camera and a 3D XCAT voxelized phantom. Right - images of the thyroid with two hot nodules (0:6 cm and 1:2 cm diameter) simulated for five collimators. Given values are the collimator spatial resolutions. Example of ROIs defined around the nodules and on the background are shown on the 3 mm SR collimator image.

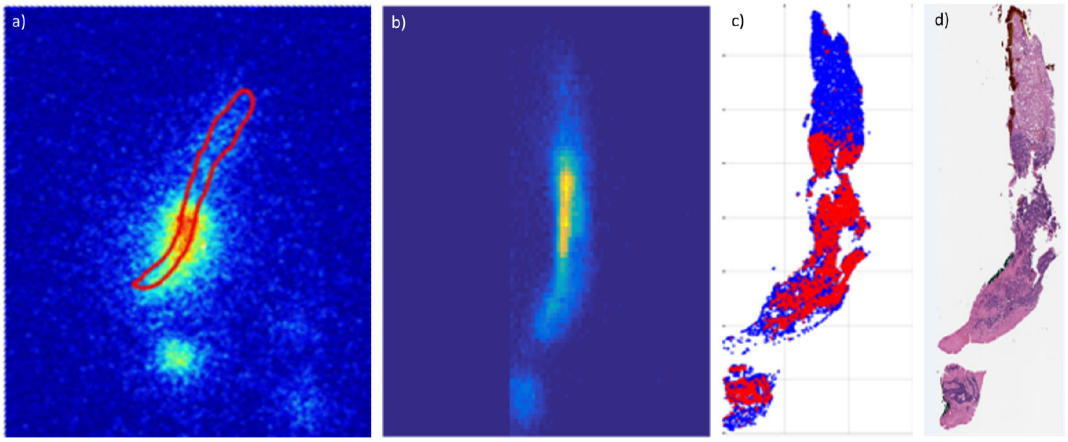

Figure 8.

Measured a) and simulated b) autoradiography (ARG) images of a liver specimen obtained from ^{18}F-FDG PET/CT guided biopsy. The simulation was performed by building within GATE a 3D voxelized source model of the distribution of tumor cells in the biopsy specimen by registering and stacking 2D slices (c, only one slice shown) in which the location of tumor cells (red) was obtained by a machine learning tool (TMARKER [168]) applied to the 58 pathology sections (d) into which the specimen was sectioned [169]. The images are not to scale and the uptake in normal liver cells (blue in c)) was set to zero for this simulation (b). Among the other factors causing a difference between the measured and simulated ARG images are deformation of the specimen during processing and inaccuracies in registration between the sections.

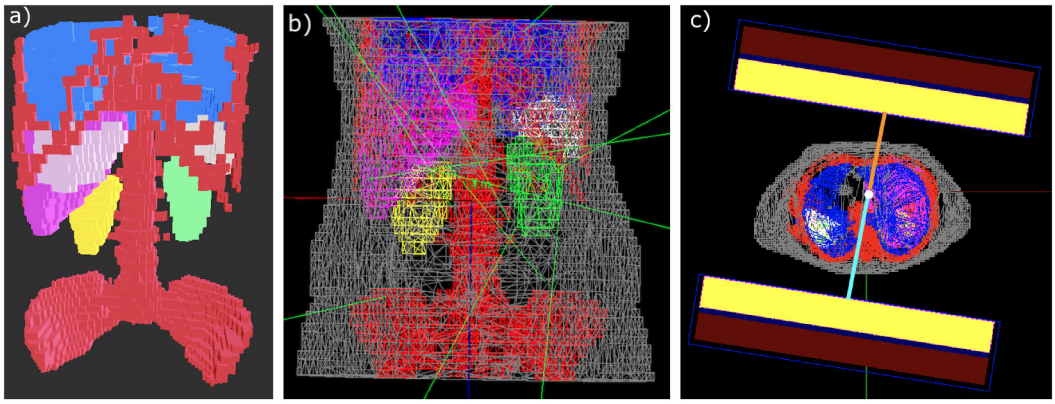

Figure 9.

a) Patient mesh model with all segmented volumes of interest: bones (red), lungs (blue), liver (pink), spleen (white) and left and right kidney (green and yellow). b) Snapshot of patient model with the remainder of the body (grey) from GATE. Few green lines represent photons emissions. c) Visualisation of the auto-contouring gamma camera motion in GATE. Unequal distances of each detector from the centre of rotation (in orange and blue respectively) shows that the camera moves in a non-circular orbit.

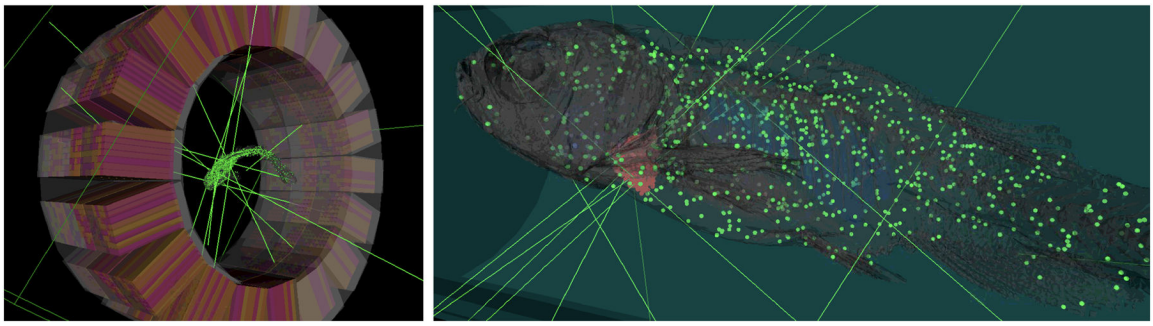

Figure 10.

3D rendering of a custom PET scanner and the MERMAID zebrafish phantom in GATE. Left: full view. Right: Zoom to the phantom, placed into a water tube. Here the grey structure represents the tessellated zebrafish volume, and the green and red dots correspond to emission locations for the entire zebrafish and the heart, respectively. The green lines indicate several representative photon trajectories.

Table 1.

Bibliography of simulated and evaluated against experimental data PET systems. LYSO: Lutetium-yttrium oxyorthosilicate, LSO: Lutetium oxyorthosilicate, BGO: Bismuth germanium oxide. The second column indicates if it is clinical (C) or preclinical (PC, for small animals) systems.

Bib. ref.	C / PC	PET system
2004 Assié et al. [7]	PC	ECAT EXACT HR+, BGO, by CPS Innovations
2004 Lazaro et al. [87]	PC	IASA prototype, CsI(Tl)
2004 Bataille et al. [10]	C	ECAT HRRT, LSO, brain
2004 Groiselle et al. [57]	C	prototype, CsI(NaI), by PhotoDetection Systems
2004 Rannou et al. [140]	PC	prototype OPET, LSO/GSO
2005 Chung et al. [27]	PC	prototype LSO and LuYAP
2005 Jan et al. [67]	C	ECAT EXACT HR+, BGO, by CTI
2006 Karakatsanis et al. [73]	C	ECAT EXACT HR+ and Biograph 2, by Siemens
2006 Lamare et al. [86]	C	Allegro/Gemini, GSO, by Philips
2006 Visvikis et al. [202]	PC	prototypes, CZT
2006 Michel et al. [112]	C	BioGraph HiRez, LSO, by Siemens
2006 Schmidtlein et al. [167]	C	Advance/Discovery Light Speed, BGO, by GE
2006 Merheb et al. [110]	PC	Mosaic, GO, by Philips
2006 Sakellios et al. [157]	PC	prototype, LSO
2006 Vandenberghe [195]	C	prototype, Univ. Penn., TOF, $LaBr_3$
2006 Vandenberghe et al. [196]	C	Allegro/Gemini, GSO, by Philips
2007 Gonias et al. [53]	C	Biograph 6, LSO, by Siemens
2007 van der Laan et al. [193]	PC	prototype, LSO
2007 Bruyndonckx et al. [17]	C	prototype, LSO
2007 Yang et al. [205]	PC	eXplore Vista, LYSO/GSO, by GE
2007 Vandervoort et al. [200]	PC	microPET R4, Focus 120, LSO, by Siemens
2007 Rey et al. [144]	PC	protoype, Lausanne ClearPET
2009 Rechka et al. [142]	PC	LabPET, LYSO, LGSO, by Sherbrooke
2009 Geramifar et al. [51]	C	Discovery DLS/DST/DSTE/DRX, BGO/LYSO, by GE
2011 McIntosh et al. [108]	PC	Inveon, LSO, by Siemens
2011 Geramifar et al. [50]	C	Discovery RX, LYSO, by GE
2012 Poon et al. [137]	C	Biograph mCT, LSO, by Siemens
2012 Trindade et al. [191]	C	Gemini TF, TruFlight Select, LYSO, by Philips
2013 Lee et al. [93]	PC	Inveon trimodal, LSO, by Siemens
2013 Nikolopoulos et al. [129]	PC	Biograph DUO, LSO, by Siemens
2013 Zagni et al. [208]	PC	Argus, LYSO/GSO, DOI, by Sedecal
2013 Solevi et al. [172]	C	prototoype AX-PET, LYSO, SiPM, brain
2015 Moraes et al. [117]	C	Biograph mCT, LSO, by Siemens
2015 Poon et al. [138]	C	Biograph mCT, LSO, by Siemens
2015 Aklan et al. [2]	C	Biograph mMR hybrid, LSO, by Siemens
2015 Monnier et al. [115]	C	Biograph mMR hybrid, LSO, by Siemens
2016 Lu et al. [103]	PC	Inveon, LSO, by Siemens

Bib. ref.	C / PC	PET system
2016 Etxebeste et al. [40]	PC	prototype, LYSO
2017 Sheikhzadeh et al. [170]	C	NeuroPET, LYSO, SiPM, brain, by PDS
2017 Li et al. [99]	C	Ray-Scan 64, BGO, by ARRAYS MIC
2018 Del Guerra et al. [35]	C	prototype TRIMAGE, LYSO
2018 Kowalski et al. [82]	C	prototype J-PET, plastic
2019 Akl et al. [1]	C	prototype PET2020, LYSO
2019 Kochebina et al. [80]	C	prototype CaLIPSO, TMBi
2020 Emami et al. [38]	C	Dual ring MAMMI breast, LYSO, by Oncovision
2020 Salvadori et al. [158]	C	Vereos, LYSO, SiPM, Philips

Table 2.

Bibliography of simulated and evaluated against experimental data SPECT systems. Collimators types are: Low Energy All Purpose (LEAR), Medium Energy General Purpose (MEGP), Low Energy High Resolution (LEHR), High Energy (HE). The second column indicates if it is clinical (C) or preclinical (PC, for small animals) systems.

Bib. ref.	C / PC	SPECT system
2003 Staelens et al. [178]	C	AXIS, LEHR/MEGP, ^{99m}Tc, ^{22}Na, ^{57}Co, ^{67}Ga, by Philips
2004 Assie et al. [6]	C	DST-Xli, MEHR, ^{111}I, by GE
2004 Assié et al. [7]	C	AXIS, LEHR/MEGP, ^{99m}Tc, by Philips
2004 Lazaro et al. [87]	PC	IASA prototype, CsI(Tl), ^{99m}Tc
2005 Staelens et al. [177]	C	IRIX, LEHR/MEGP, ^{99m}Tc, by Philips
2005 Autret et al. [8]	C	DST-XLi, Millennium VG, ^{131}I, by GE
2006 Staelens et al. [179]	PC	ECAM multi-pinhole, ^{123}I, by Siemens
2006 Vandenberghe et al. [197]	PC	prototype SOLSITCE, solid-state, CZT, ^{99m}Tc
2006 Sakellios et al. [157]	PC	prototype, PSPMT, CsI(Tl), ^{99m}Tc
2008 Carlier et al. [23]	C	Symbia, ^{99m}Tc, ^{111}I, ^{131}I, by Siemens
2009 Park et al. [132]	PC	TRIAD XLT9, LEUHR, NaI(Tl), ^{99m}Tc, by Trionix
2010 Mok et al. [114]	PC	XSPECT, multi-pinhole, ^{99m}Tc, by Gamma Medica-Ideas
2011 Robert et al. [149]	C	prototype, HiSens, CZT, LEHR/H13, ^{99m}Tc, ^{57}Co
2011 Boisson et al. [14]	PC	prototype, parallel slat, YAP:Ce, ^{99m}Tc, ^{57}Co
2015 Lee et al. [95]	PC	Symbia T2, LEAP/LEHR/HE, ^{131}I, ^{99m}Tc, by Siemens
2015 Lee et al. [94]	PC	Inveon, LSO, ^{123}I, ^{125}I, by Siemens
2015 Spirou et al. [176]	C	ECAM, NaI(Tl), ^{99m}Tc, by Siemens
2017 Georgiou et al. [49]	PC	γ-eye, CsI(Na), ^{99m}Tc, ^{111}In, ^{177}Lu, by Bioemtech
2017 Costa et al. [30]	C	Symbia T2, MEAP, ^{177}Lu, by Siemens
2018 Taherparvar et al. [187]	PC	prototype, CsI(Na), ^{99m}Tc
2019 Sadremomtaz et al. [155]	PC	HiReSPECT, LEHR, CsI(Na), ^{99m}Tc, by PNP